DROPLET FOOTPRINT CONTROL*

ANTOINE LAURAIN† AND SHAWN W. WALKER‡

Abstract. Controlling droplet shape via surface tension has numerous technological applications, such as droplet lenses and lab-on-a-chip. This motivates a partial differential equation-constrained shape optimization approach for controlling the shape of droplets on flat substrates by controlling the surface tension of the substrate. We use shape differential calculus to derive an L^2 gradient flow approach to compute equilibrium shapes for sessile droplets on substrates. We then develop a gradient-based optimization method to find the substrate surface tension coefficient yielding an equilibrium droplet shape with a desired *footprint* (i.e., the liquid-solid interface has a desired shape). Moreover, we prove a sensitivity result with respect to the substrate surface tensions for the free boundary problem associated with the footprint. Numerical results are also presented to showcase the method.

Key words. control of free boundary, bilevel shape optimization, droplet shape control, surface tension

AMS subject classifications. Primary, 35R35, 49Q10; Secondary, 35Q93

DOI. 10.1137/140979721

1. Introduction. The development of engineered substrates has progressed to a very advanced level [4, 45, 52, 58, 41, 59], which allows for control of the shape of sessile droplets on these substrates. Controlling local droplet shape via substrate surface tensions may be useful for directing the growth of bio-films and cell cultures as it can affect the distribution of nutrients as well as the gross shape of the film [8, 20, 21, 44, 55, 78]. In addition, depositing a film of material onto a substrate [28, 39, 46] in a particular pattern could be affected by the droplet shape. Also, droplets can act as lenses, with focal properties controlled by locally modifying substrate tensions [9, 54, 34].

The problem of finding the shape of the droplet is a free boundary problem, i.e., the boundary of the droplet is determined by the solution of a partial differential equation involving geometric quantities defining the geometry such as the total curvature (i.e., sum of principle curvatures) and the contact angle with the substrate. Usually an analytical solution of the free boundary problem is not available and an optimization approach can be used to find an approximation of the free boundary. The free boundary also depends on certain physical parameters that can be used to control its shape. In this paper, we actually propose an optimal control for the shape of droplets on substrates. Specifically, we wish to direct the shape of the droplet-substrate interface (i.e., the liquid-solid interface) by controlling the substrate surface tension. We refer to this as *droplet footprint control*.

This control problem can be modeled as a bilevel shape optimization problem, where the free boundary problem constitutes the lower-level optimization problem and the upper-level consists in minimization with respect to substrate surface tension. Control of free boundaries has seldom been considered in shape optimization due to the inherent complexity. In [60, section 4.3.2] shape controllability of the free boundary of an obstacle problem is studied; see also [31, 32]. In [63, 64], shape and topology optimization of Bernoulli free boundary problems are considered. Shape optimization problems in fluid dynamics governed by free surface flows are considered in [37], where a sensitivity analysis of the free surface problem with the Navier–Stokes equations as constraints is formally studied. See also [38] for a rigorous mathematical analysis for bilevel Bernoulli problems. In the present work, we carry out the shape sensitivity analysis of the free boundary with respect to the substrate surface tension in the infinite-dimensional setting using the tools of shape calculus [16, 60]. For this purpose we introduce two cost functionals to drive the free boundary as close as possible to a given desired set.

Concerning the numerical realization of the bilevel optimization problem, a possible approach consists in replacing the free boundary constraint by a penalization of the cost functional on the upper-level problem, which allows us to bypass the solution of the free boundary problem. Unfortunately, as noted in [63], this approach leads to serious convergence problems and a locally optimal solution might not represent a physical solution to the free boundary problem. In our approach, we solve the lower-level (forward) problem to steady state (using a gradient flow) to obtain the droplet shape for a given surface tension. The upper-level optimization problem is solved by a gradient descent scheme posed in function space. See [71, 75] for related descent schemes.

The outline of the paper is the following. We start in section 2 with a reminder of the notion of shape derivative and give useful formulae of integration by parts on surfaces and for the shape derivative of typical shape functionals. In section 3 the equilibrium equations determining the shape of the droplet are derived. In section 4 the bilevel optimization problem is introduced, and the sensitivity of the free boundary with respect to the surface tension is performed. Finally, the shape derivative of the two functionals used to drive the free boundary toward a desired footprint shape are computed with the previous results. In section 5 an iterative algorithm to compute the free boundary and to solve the upper-level problem is described and numerical results are given.

2. Shape sensitivity.

2.1. Perturbation of identity. In this paper concepts of shape differential calculus, described in detail in [16, 30, 51, 60], are utilized. The inherent difficulty in dealing with shape functionals lies in the fact that sets of shapes are not vector spaces and the notion of differentiation cannot be used directly. Instead, one may consider perturbations of a reference shape by means of transformations in an appropriate function space which allows differentiation of the functional. These transformations can be constructed, for instance, by perturbation of the identity [16] or by the flow of a velocity field [16, 60]. We will use the perturbation of identity method in what follows.

To this end let $\mathcal{C}_b^k(\mathbb{R}^n, \mathbb{R}^n)$ be the space of k-times continuously differentiable vector-valued functions $\mathbf{V}$ with $D^\beta \mathbf{V}$ bounded whenever $0 \leq |\beta| \leq k$, where β is a multi-index, and equipped with the standard $\mathcal{C}^k$-norm. We write $\mathcal{C}_b^{k,\alpha}(\mathbb{R}^n, \mathbb{R}^n)$,

$k \geq 2$, $0 < \alpha \leq 1$, for the space of functions $\mathbf{V} \in \mathcal{C}_b^k(\mathbb{R}^n, \mathbb{R}^n)$ such that $D^\beta \mathbf{V}$ is Hölder continuous with exponent α whenever $|\beta| = k$. The space $\mathcal{C}_b^{k,\alpha}(\mathbb{R}^n, \mathbb{R}^n)$, equipped with the norm

$$\|\mathbf{V}\|_{k,\alpha} := \sum_{|\beta| \leq k} \sup |D^\beta \mathbf{V}| + \sum_{|\beta|=k} \sup_{x,y,x\neq y} \frac{|D^\beta \mathbf{V}(x) - D^\beta \mathbf{V}(y)|}{|x-y|^\alpha},$$

is a Banach space.

We consider perturbations of identity $I + \mathbf{V}$ where $\mathbf{V}$ is in a neighborhood of 0 in $\mathcal{C}_b^{k,\alpha}(\mathbb{R}^n, \mathbb{R}^n)$ so that $I + \mathbf{V}$ is a bi-Lipschitz homeomorphism. In what follows we will denote by

$$\mathcal{S}_{\mathbf{V}} := (I + \mathbf{V})(\mathcal{S})$$

the transformation of a generic domain $\mathcal{S} \subset \mathbb{R}^n$ by $I + \mathbf{V}$. Let $K(\Omega)$ be a real-valued functional associated with $\Omega \subset \mathbb{R}^n$. The functional $K(\Omega)$ is Fréchet-differentiable at Ω if there exists a bounded linear operator $\nabla K(\Omega)$ from $\mathcal{C}_b^{k,\alpha}(\mathbb{R}^n, \mathbb{R}^n)$ to $\mathbb{R}$ called *shape gradient* such that

$$K(\Omega_{\mathbf{V}}) = K(\Omega) + \nabla K(\Omega) \cdot \mathbf{V} + r(\mathbf{V}),$$

where $|r(\mathbf{V})|/\|\mathbf{V}\|_{k,\alpha} \to 0$ as $\|\mathbf{V}\|_{k,\alpha} \to 0$. In this case one defines the *shape derivative* as

$$(2.1) \qquad\qquad \delta K(\Omega; \mathbf{V}) := \nabla K(\Omega) \cdot \mathbf{V}.$$

Sometimes the notation $\delta_\Omega K(\Omega; \mathbf{V})$ will also be used for the shape derivative, typically when K takes several arguments. According to the structure theorem of Hadamard and Zolésio [16],

$$(2.2) \qquad\qquad \mathcal{C}_b^{k,\alpha}(\mathbb{R}^n, \mathbb{R}^n) \ni \mathbf{V} \mapsto \delta K(\Omega; \mathbf{V})$$

is a distribution on $\mathbb{R}^n$ with support on $\partial\Omega$.

A similar definition can be used for the shape derivative of functionals taking their values in a Banach space. In particular, an interesting case is to define the shape derivative of the solution of a partial differential equation. Let $f(\Omega_{\mathbf{V}})$, also denoted $f_{\mathbf{V}}$, be such a function depending on the perturbed domain $\Omega_{\mathbf{V}}$. Since $f_{\mathbf{V}}$ lives in a function space which depends on the moving domain $\Omega_{\mathbf{V}}$, it is not clear how to compute the shape derivative directly. Instead one takes the derivative of $f_{\mathbf{V}} \circ (I + \mathbf{V})$, which is defined on Ω, with respect to $\mathbf{V}$ in a direction $\widehat{\mathbf{V}}$; the latter is called *material derivative* and written $D_\Omega f(\mathbf{V}; \widehat{\mathbf{V}})$ or $D_\Omega f(\Omega; \widehat{\mathbf{V}})$ if $\mathbf{V} \equiv 0$. Then one defines the *shape derivative* by

$$(2.3) \qquad\qquad \delta_\Omega f(\mathbf{V}; \widehat{\mathbf{V}}) := D_\Omega f(\mathbf{V}; \widehat{\mathbf{V}}) - \nabla f \cdot \widehat{\mathbf{V}}.$$

Since one usually considers $\delta_\Omega f(0; \widehat{\mathbf{V}})$, the notation $\delta_\Omega f(\Omega, \widehat{\mathbf{V}}) := \delta_\Omega f(0; \widehat{\mathbf{V}})$ or $\delta_\Omega f(\widehat{\mathbf{V}}) := \delta_\Omega f(0; \widehat{\mathbf{V}})$ is also used for readability when no confusion is possible.

2.2. Integration by parts relations. In the rest of the paper we take $n = 3$. We use a subscript on ∇ to denote the domain on which the gradient is computed. For instance, if Γ is a surface in $\mathbb{R}^3$, then ∇_Γ is the gradient operator *on* Γ, i.e., ∇_Γ is the surface gradient [16, 60]. Furthermore, we have the "surface Laplacian" (or

Laplace–Beltrami) operator $\Delta_\Gamma = \nabla_\Gamma \cdot \nabla_\Gamma$. We note the following essential calculus results from [16, 60, 67, 68]. (See Figure 1 for an illustration of various geometric terms.)

PROPOSITION 2.1. *Let Γ be a two-dimensional surface of class $\mathcal{C}^{k,\alpha}$ embedded in $\mathbb{R}^3$ with unit normal vector $\boldsymbol{\nu}$. If Γ is a surface with boundary (also called an open surface), we assume its boundary $\partial\Gamma$ is of class $\mathcal{C}^{k,\alpha}$. Let κ be the* total *curvature of Γ (sum of the principal curvatures) such that $\kappa\boldsymbol{\nu} := -\Delta_\Gamma \mathrm{id}_\Gamma$, where $\mathrm{id}_\Gamma : \Gamma \to \Gamma$ is the identity map on Γ. If Γ is closed, assume $\boldsymbol{\nu}$ points* outward*; this implies that κ is positive when Γ is strictly convex. If Γ is open, then let $\boldsymbol{\tau}$ be the positively oriented tangent vector of $\partial\Gamma$ (with respect to $\boldsymbol{\nu}$) and define $\mathbf{b} : \partial\Gamma \to \mathbb{R}^3$ as*

$$(2.4) \qquad \mathbf{b} = \boldsymbol{\tau} \times \boldsymbol{\nu},$$

where $\mathbf{b}$ points out of the surface Γ. Then we have

$$(2.5) \qquad \int_\Gamma [\nabla_\Gamma \omega]^T = \int_\Gamma \omega\kappa\boldsymbol{\nu} + \int_{\partial\Gamma} \omega\mathbf{b}$$

for all scalar $\omega \in H^1(\Gamma, \mathbb{R})$.

PROPOSITION 2.2. *Under the same assumptions as in Proposition* 2.1*, we have the relations*

$$(2.6) \qquad \int_\Gamma \nabla_\Gamma \boldsymbol{\varphi} = \int_\Gamma \boldsymbol{\varphi} \otimes \boldsymbol{\nu}\, \kappa + \int_{\partial\Gamma} \boldsymbol{\varphi} \otimes \mathbf{b},$$

$$(2.7) \qquad \int_\Gamma \nabla_\Gamma \cdot \boldsymbol{\varphi} = \int_\Gamma \boldsymbol{\varphi} \cdot \boldsymbol{\nu}\kappa + \int_{\partial\Gamma} \boldsymbol{\varphi} \cdot \mathbf{b}$$

for all vector functions $\boldsymbol{\varphi} \in H^1(\Gamma, \mathbb{R}^3)$.

2.3. Shape derivative formulae. Let Ω be a domain in $\mathbb{R}^3$ of class $\mathcal{C}^{k,\alpha}$ and define a functional

$$J_1(\Omega) := \int_\Omega f(\Omega)(x)dx,$$

where $f(\Omega) \in H^1(\Omega, \mathbb{R})$ is a function defined on Ω that may also depend on the shape of Ω. For $\mathbf{V} \in \mathcal{C}_b^{k,\alpha}(\mathbb{R}^3, \mathbb{R}^3)$, the shape derivative of J_1 is given by [16, 60]

$$(2.8) \qquad \delta J_1(\Omega; \mathbf{V}) = \int_\Omega \delta_\Omega f(\Omega; \mathbf{V}) + \int_{\partial\Omega} f(\Omega)\mathbf{V} \cdot \boldsymbol{\nu}.$$

Next, consider an open surface $\Gamma \subset \mathbb{R}^3$ of class $\mathcal{C}^{k,\alpha}$ with boundary $\Sigma \equiv \partial\Gamma \subset \mathcal{P}$ also of class $\mathcal{C}^{k,\alpha}$, where $\mathcal{P}$ is the plane $\mathbb{R}^2 \times \{z = 0\}$ (see Figure 1); note that Σ is a closed curve in $\mathcal{P}$. Define the functionals

$$Q_0(\Gamma) := \int_\Gamma f(\Omega), \qquad Q_1(\Gamma) := \int_\Gamma g(\Gamma), \qquad Q_2(\Gamma) := \int_\Sigma g(\Gamma),$$

where $f(\Omega) \in H^1(\Omega, \mathbb{R})$ and $g(\Gamma) \in H^1(\Gamma, \mathbb{R})$ is a function defined on Γ that also depends on the shape of Γ. The shape derivative of Q_0 can be derived from [16, 60]

$$(2.9) \qquad \begin{aligned} \delta Q_0(\Gamma; \mathbf{V}) &= \int_\Gamma \delta_\Omega f(\Omega; \mathbf{V}) + (\mathbf{V} \cdot \nabla)f + f(\nabla_\Gamma \cdot \mathbf{V}) \\ &= \int_\Gamma \delta_\Omega f(\Omega; \mathbf{V}) + [(\boldsymbol{\nu} \cdot \nabla)f + f\kappa](\mathbf{V} \cdot \boldsymbol{\nu}) + \int_\Sigma f\mathbf{b} \cdot \mathbf{V}. \end{aligned}$$

Functionals $Q_1(\Gamma)$ and $Q_2(\Gamma)$ are integrals on lower-dimensional subsets of the ambient space $\mathbb{R}^3$, i.e., integrals over a surface or a curve. The integrand $g(\Gamma)$ needs to be extended to a neighborhood of Γ in order to compute the shape derivatives of $Q_1(\Gamma)$ and $Q_2(\Gamma)$. Obviously, the shape derivatives of $Q_1(\Gamma)$ and $Q_2(\Gamma)$ and the material derivative of $g(\Gamma)$ defined in section 2.1 are both independent of this extension.

However, one observes from the definition (2.3) that the shape derivative of $g(\Gamma)$ depends on this extension due to the presence of ∇g. This particularity is often hidden in shape optimization since one conveniently considers a unitary extension along the normal, so that the term $\nabla g \cdot \widehat{\mathbf{V}}$ in (2.3) vanishes when $\widehat{\mathbf{V}}$ is normal to the submanifold. This corresponds to the derivative of $Q_1(\Gamma)$; see (2.10).

Nevertheless, we are facing an unusual situation when computing the shape derivative of $Q_2(\Gamma)$. Indeed, in our paper the curve Σ is constrained to stay in the plane $\mathcal{P}$ and is consequently not perturbed in the direction normal to the surface Γ. In this particular case, it is preferable to use a unitary extension along the normal vector $\mathbf{b}_\mathrm{s}$ to Σ inside the plane $\mathcal{P}$.

Thus we use *two different extensions* which lead to *two different notions* of shape derivatives for functions taking their values in a Banach space. In order to distinguish them, we use the notation $\delta_\Omega g(\Gamma; \mathbf{V})$ for the so-called space shape derivative of $g(\Gamma)$ when using a unitary extension along the normal vector $\boldsymbol{\nu}$ to Γ and the notation $\delta_\Omega^{\mathcal{P}} g(\Gamma; \mathbf{V})$ for the so-called $\mathcal{P}$-shape derivative when using a unitary extension along $\mathbf{b}_\mathrm{s}$ in the plane $\mathcal{P}$. This distinction is not important for the final result which should be independent of the extensions, but it is important for the calculations and proofs leading to the final result.

The shape derivative of Q_1 using a constant extension of $g(\Gamma)$ along the normal $\boldsymbol{\nu}$ follows from [16, 60]:

(2.10)
$$\delta Q_1(\Gamma; \mathbf{V}) = \int_\Gamma \delta_\Omega g(\Gamma; \mathbf{V}) + (\mathbf{V} \cdot \nabla_\Gamma) g + g(\nabla_\Gamma \cdot \mathbf{V}) = \int_\Gamma \delta_\Omega g(\Gamma; \mathbf{V}) + \nabla_\Gamma \cdot (g\mathbf{V})$$
$$= \int_\Gamma \delta_\Omega g(\Gamma; \mathbf{V}) + g\kappa(\mathbf{V} \cdot \boldsymbol{\nu}) + \int_\Sigma g\, \mathbf{b} \cdot \mathbf{V},$$

with respect to a general flow velocity $\mathbf{V}$, where κ is the signed total curvature of Γ.

As for Q_2, we adopt a unitary extension of $g(\Gamma)$ along the normal $\mathbf{b}_\mathrm{s}$ to Σ inside the plane $\mathcal{P}$, and this yields the formula

$$\delta Q_2(\Gamma; \mathbf{V}) = \int_\Sigma \delta_\Omega^{\mathcal{P}} g(\Gamma; \mathbf{V}) + (\mathbf{V} \cdot \nabla_{\mathcal{P}}) g + g(\nabla_\Sigma \cdot \mathbf{V})$$

for all flow velocities $\mathbf{V}$ restricted to the plane $\mathcal{P}$. If the contact angle of Γ with respect to $\mathcal{P}$ is bounded away from 0 and π, then we have

(2.11)
$$\delta Q_2(\Gamma; \mathbf{V}) = \int_\Sigma \delta_\Omega^{\mathcal{P}} g(\Gamma; \mathbf{V}) + (\mathbf{V} \cdot \nabla_\Sigma) g + g(\nabla_\Sigma \cdot \mathbf{V})$$
$$= \int_\Sigma \delta_\Omega^{\mathcal{P}} g(\Gamma; \mathbf{V}) + g\, \kappa_\Sigma (\mathbf{V} \cdot \mathbf{b}_\mathrm{s})$$

for all flow velocities $\mathbf{V}$ restricted to the plane $\mathcal{P}$, where κ_Σ is the signed curvature of Σ. Since Σ is a curve, one can show that $\nabla_\Sigma \equiv \boldsymbol{\tau}\, \partial_s$, where ∂_s is the derivative with respect to arc-length on Σ and $\boldsymbol{\tau}$ is the unit tangent vector of Σ.
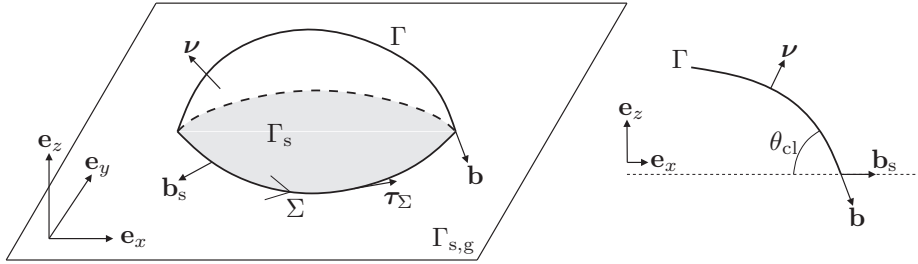
FIG. 1. *Illustration of a droplet on a flat solid substrate. The volume region of the droplet is denoted Ω, and the boundary decomposes as $\overline{\partial\Omega} = \overline{\Gamma} \cup \overline{\Gamma_s}$, where Γ is the liquid-gas interface and Γ_s is the liquid-solid interface (shaded). The solid-gas interface is labeled $\Gamma_{s,g}$. The plane of the substrate is the x,y plane $\mathbb{R}^2$ and is denoted $\mathcal{P} \equiv \overline{\Gamma_s} \cup \overline{\Gamma_{s,g}}$. The contact line is denoted Σ, is defined by $\Sigma = \overline{\Gamma} \cap \overline{\Gamma_s}$, and is oriented with unit tangent vector $\boldsymbol{\tau}_\Sigma$. The unit outer normal to Ω is denoted $\boldsymbol{\nu}$ on Γ, $\boldsymbol{\nu}_s \equiv -\mathbf{e}_z$ on Γ_s, and $\boldsymbol{\nu}_{s,g} \equiv -\mathbf{e}_z$ on $\Gamma_{s,g}$. The open surface Γ has outward unit boundary vector $\mathbf{b}$ defined only on $\Sigma \equiv \partial\Gamma$; likewise, Γ_s has boundary vector $\mathbf{b}_s$ which points in the $\mathcal{P}$ plane. The contact angle at Σ is denoted θ_{cl}, where $\cos\theta_{cl} = \mathbf{b} \cdot \mathbf{b}_s$.*

3. Equilibrium droplets attached to surfaces.
We wish to optimize the shape of droplets that are in equilibrium with respect to surface tension forces and, possibly, other physical effects such as gravity. This section describes the so-called forward (or lower-level) problem in our optimization.

3.1. Constrained droplet.
Let Ω be a three-dimensional droplet sitting on a flat substrate, as shown in Figure 1. The entire plane of the substrate is denoted $\mathcal{P} := \mathbb{R}^2 \times \{z = 0\}$. Consider the equilibrium configuration of the droplet Ω. The relevant free energy for this problem is

$$(3.1) \qquad \mathcal{A}(\Omega) = \int_{\Gamma_s} \gamma_s + \int_\Gamma \gamma + \int_{\Gamma_{s,g}} \gamma_{s,g} - \rho\mathbf{g} \cdot \int_\Omega (\mathbf{x} - \mathbf{x}_0),$$

where $\mathbf{g}$ is the vector acceleration due to gravity and $\gamma_s \in \mathcal{C}_b^{k+1,\alpha}(\mathcal{P})$, $\gamma_{s,g} \in \mathcal{C}_b^{k+1,\alpha}(\mathcal{P})$ and $\gamma \in \mathbb{R}$ are surface tension coefficients for the different interfaces. We assume Ω and the interfaces $\Gamma_s, \Gamma, \Gamma_{s,g}$ are of class $\mathcal{C}^{k+1,\alpha}$.

Note that the "dry" part of $\mathcal{P}$ is denoted by $\Gamma_{s,g}$, and the "wet" part of $\mathcal{P}$ is Γ_s. Most material surfaces have a surface tension coefficient which depends on the adjoining material [14, 15], i.e., the surface tension in the solid-gas region, $\gamma_{s,g}$, is different from the surface tension in the liquid-solid region, γ_s. Note that $\gamma_{s,g}$ and γ_s are defined in the entire plane but are active only in $\Gamma_{s,g}$ and Γ_s, respectively. These two coefficients, which may be spatially varying, could be used as control functions to direct the shape of the droplet. In other words, changing $\gamma_{s,g}$ and γ_s induces a change in the equilibrium shape of Ω (see the boundary condition in (3.9)).

To facilitate deriving the equilibrium equations for the *shape* of the droplet, we introduce the Lagrangian

$$(3.2) \qquad \mathcal{L}(\Omega, p_0) = \mathcal{A}(\Omega) - p_0 \left(\int_\Omega 1 \, d\mathbf{x} - C_p \right),$$

which includes the volume constraint $|\Omega| = C_p$ via the Lagrange multiplier $p_0 \in \mathbb{R}$.

3.2. Equilibrium conditions.
Let $\mathbf{V} \in \mathcal{C}_b^{k,\alpha}(\mathbb{R}^3, \mathbb{R}^3)$ be a vector field that vanishes at a large distance from Ω. We will perturb the domain Ω with $\mathbf{V}$. Furthermore, we restrict $\mathbf{V}$ such that $\mathbf{V} \cdot \mathbf{e}_z = -\mathbf{V} \cdot \boldsymbol{\nu}_s = 0$ on the rigid substrate $\mathcal{P}$. In other words, we consider vector fields in the space

$$\mathbf{V} \in \mathcal{V} := \{\mathbf{W} \in \mathcal{C}_b^{k,\alpha}(\mathbb{R}^3, \mathbb{R}^3), \mathbf{W} \cdot \mathbf{e}_z = 0 \text{ on } \mathcal{P}\}.$$

Next, apply (2.8) and the first line of formula (2.10) to compute the shape derivative of $\mathcal{L}(\Omega)$:

$$(3.3) \quad \delta_\Omega \mathcal{L}(\Omega, p_0; \mathbf{V}) = \int_{\Gamma_s} \nabla_{\Gamma_s} \cdot (\gamma_s \mathbf{V}) + \int_\Gamma \nabla_\Gamma \cdot (\gamma \mathbf{V}) + \int_{\Gamma_{s,g}} \nabla_{\Gamma_{s,g}} \cdot (\gamma_{s,g} \mathbf{V})$$
$$- \rho \mathbf{g} \cdot \int_{\partial\Omega} (\mathbf{x} - \mathbf{x}_0)(\mathbf{V} \cdot \boldsymbol{\nu}) - p_0 \int_\Gamma \mathbf{V} \cdot \boldsymbol{\nu},$$

where we have used the fact that $\gamma_s, \gamma, \gamma_{s,g}$, and g are independent of the shape Ω. Next, after integration by parts, i.e., applying Proposition 2.2, and using $\mathbf{V} \cdot \mathbf{e}_z = 0$, (3.3) reduces to

$$\delta_\Omega \mathcal{L}(\Omega, p_0; \mathbf{V}) = \int_{\partial\Gamma_s} \gamma_s \mathbf{V} \cdot \mathbf{b}_s + \int_{\partial\Gamma} \gamma \mathbf{V} \cdot \mathbf{b} + \int_{\partial\Gamma_{s,g}} \gamma_{s,g} \mathbf{V} \cdot \overbrace{\mathbf{b}_{s,g}}^{=-\mathbf{b}_s} - p_0 \int_\Gamma \mathbf{V} \cdot \boldsymbol{\nu}$$

$$(3.4) \qquad + \int_{\Gamma_s} \gamma_s \kappa_s \boldsymbol{\nu}_s \cdot \mathbf{V} + \int_\Gamma \gamma \kappa \boldsymbol{\nu} \cdot \mathbf{V} + \int_{\Gamma_{s,g}} \gamma_{s,g} \kappa_{s,g} \boldsymbol{\nu}_{s,g} \cdot \mathbf{V}$$

$$- \rho \mathbf{g} \cdot \int_\Gamma (\mathbf{x} - \mathbf{x}_0)(\mathbf{V} \cdot \boldsymbol{\nu}),$$

where κ_j is the total curvature (sum of the principle curvatures) of Γ_j ($j = s$ or (s,g)), and $\kappa_j \boldsymbol{\nu}_j = -\Delta_{\Gamma_j} \mathrm{id}_{\Gamma_j}$, where $\mathrm{id}_{\Gamma_j} : \Gamma_j \to \Gamma_j$ is the identity map on Γ_j [16, 60, 67, 68]. We reserve κ to refer to the total curvature of Γ. The restriction $\mathbf{V} \in \mathcal{V}$ implies $\boldsymbol{\nu}_{s,g} \cdot \mathbf{V} = \boldsymbol{\nu}_s \cdot \mathbf{V} = 0$ on $\Gamma_{s,g}$ and Γ_s. Accounting for the geometry of the interfaces and the contact line, we arrive at

$$\delta_\Omega \mathcal{L}(\Omega, p_0; \mathbf{V}) = \int_\Sigma (\gamma_s - \gamma_{s,g}) \mathbf{V} \cdot \mathbf{b}_s + \int_\Sigma \gamma \mathbf{V} \cdot \mathbf{b}$$

$$(3.5) \qquad + \int_\Gamma (\gamma \kappa - \rho \mathbf{g} \cdot (\mathbf{x} - \mathbf{x}_0) - p_0) \mathbf{V} \cdot \boldsymbol{\nu}.$$

At equilibrium, we must have $\delta_\Omega \mathcal{L}(\Omega, p_0; \mathbf{V}) = 0$ for all admissible $\mathbf{V} \in \mathcal{V}$. Since we have assumed Γ is of class $\mathcal{C}^{k+1,\alpha}$, we have $\boldsymbol{\nu}$ of class $\mathcal{C}^{k,\alpha}$. Thus, we can take $\mathbf{V} = \phi \boldsymbol{\nu} \in \mathcal{V}$, where ϕ is in $\mathcal{C}^{k,\alpha}(\Gamma, \mathbb{R})$ with compact support on Γ, and plug into (3.5) to obtain

$$(3.6) \qquad \delta_\Omega \mathcal{L}(\Omega, p_0; \mathbf{V}) = \int_\Gamma (\gamma \kappa - \rho \mathbf{g} \cdot (\mathbf{x} - \mathbf{x}_0) - p_0) \phi = 0,$$

and thus

$$(3.7) \qquad \gamma \kappa - \rho \mathbf{g} \cdot (\mathbf{x} - \mathbf{x}_0) - p_0 = 0 \text{ on } \Gamma,$$

which is a PDE that determines the shape of Γ, and also $p_0 \in \mathbb{R}$. Note that this means that $\gamma \kappa - \rho \mathbf{g} \cdot (\mathbf{x} - \mathbf{x}_0)$ must be a constant as $p_0 \in \mathbb{R}$.

Next take $\mathbf{V}$ such that $\mathbf{V} = \phi \mathbf{b}_s$ on Σ, with $\phi \in \mathcal{C}^{k,\alpha}(\Sigma, \mathbb{R})$, and note that $\cos \theta_{cl} = \mathbf{b} \cdot \mathbf{b}_s$. Then, taking into account the equilibrium condition (3.7), equation (3.5) reduces to

$$(3.8) \qquad \delta_\Omega \mathcal{L}(\Omega, p_0; \mathbf{V}) = \int_\Sigma (\gamma \cos \theta_{cl} + \gamma_s - \gamma_{s,g}) \phi.$$

Therefore, at equilibrium, suitable choices of the "test" perturbation $\mathbf{V}$ yield

(3.9) $\gamma \cos \theta_{\mathrm{cl}} + \gamma_{\mathrm{s}} - \gamma_{\mathrm{s,g}} = 0$ on Σ,

which is the corresponding boundary condition for (3.7).

Remark 3.1.   Equation (3.9) is the classic Young–Laplace relation.   Finally, note that the derivative of $\mathcal{L}(\Omega, p_0)$ with respect to p_0 provides the volume constraint $|\Omega| = C_p$ for Ω.

3.3. Lower-level problem formulation.   In order to render the rest of the paper more readable we make the following assumptions and notational simplifications, which do not affect the main ideas of the study:

- Set $\gamma = 1$ and $\rho = 1$.
- Set $G(\mathbf{x}) := \mathbf{g} \cdot (\mathbf{x} - \mathbf{x}_0)$.
- Let $u = (\gamma_{\mathrm{s}} - \gamma_{\mathrm{s,g}})|_\Sigma$ be a given fixed function (the *control*) defined on the contact line (Σ). In order to be consistent with (3.9), we assume that $|u| < 1$.
- We assume $u \in \mathcal{C}^{k+1,\alpha}(\Sigma, \mathbb{R})$.

Next, using these simplifications, we rewrite (3.5) for convenience. The problem is to find Γ and $p_0 \in \mathbb{R}$ such that

(3.10)

$$\delta_\Omega \mathcal{L}(\Omega, p_0; \mathbf{V}) = \int_\Sigma u \, \mathbf{b}_{\mathrm{s}} \cdot \mathbf{V} + \int_\Sigma \mathbf{b} \cdot \mathbf{V} + \int_\Gamma \kappa \boldsymbol{\nu} \cdot \mathbf{V} - \int_\Gamma G \boldsymbol{\nu} \cdot \mathbf{V} - p_0 \int_\Gamma \boldsymbol{\nu} \cdot \mathbf{V} = 0,$$

$$\int_\Omega 1 = C,$$

for all $\mathbf{V} \in \mathcal{V}$.

Remark 3.2.   The well-posedness of (3.10) (equivalently, (3.7) and (3.9)) is nontrivial. Assuming Σ is given (fixed) and $G \equiv 0$; then the minimization problem reduces to a surface of constant mean curvature with fixed open boundary. Existence of this problem has been studied in [61, 76] (see also [2, 29]). Allowing for Σ to be free, there is early work on minimal surfaces (zero mean curvature) with a free boundary having a contact angle of 90° [13, 36, 49] and more recently on the volume constrained (constant mean curvature) case [11, 25, 62, 56].

Capillary surfaces [15, 26] of variable contact angle, e.g., not equal to 90°, are an active field of research [1, 12, 48, 57] and many questions are open regarding the existence of equilibrium shapes for contact angles between 90° and 180°. Moreover, including G complicates the problem further; see Remark 4.3. In view of the existing results, it is nevertheless reasonable to conjecture the existence and uniqueness of a solution to (3.10) required for deriving our shape control results. Therefore we make the following assumption.

Assumption 3.3.   For each admissible $u \in \mathcal{C}^{k+1,\alpha}(\Sigma, \mathbb{R})$, there exists a unique $\mathcal{C}^{k+1,\alpha}$ surface Γ, with boundary Σ of class $\mathcal{C}^{k+1,\alpha}$, and p_0 in $\mathbb{R}$ such that (3.10) is true for all $\mathbf{V} \in \mathcal{V}$. Note also that Γ implicitly defines Γ_{s}.

4. Optimization of surface droplets.   In this section we introduce the bilevel problem for controlling the free boundary using u. To this aim we analyse two cost functionals measuring the distance between the free boundary and some desired set. The distance between two sets can be measured in various ways, and here we consider two possibilities: the first one is the L^2-distance between the characteristic functions of two sets, and the second one is based on the distance function to the target set.

In order to compute the derivative of the cost function with respect to u, we need to study the sensitivity of the free boundary with respect to this control. We show that a variation of the control corresponds to a perturbation of the free boundary in the direction of a vector field whose existence is proved in section 4.3. Its derivative, which is useful to compute the derivative of the cost functional, is also given in (4.26)–(4.27).

4.1. Optimization problem. Let $\chi : \mathcal{P} \to \{0,1\}$ denote characteristic functions defined over the solid substrate. Let Γ_d represent a desired shape for the liquid-solid interface Γ_s and $\chi_{\{\Gamma_d\}}$ be its indicator function. Consider a cost functional $J(\Gamma_s)$ measuring the distance between Γ_s and Γ_d. An example of such a functional is

$$(4.1) \qquad J(\Gamma_s) = \frac{1}{2} \int_{\mathcal{P}} (\chi_{\{\Gamma_s\}} - \chi_{\{\Gamma_d\}})^2.$$

When Γ_s is the free boundary solution of (3.7) and (3.9) or equivalently solves the variational problem (3.10), then it depends on the substrate surface tension control function $u = (\gamma_s - \gamma_{s,g})|_\Sigma$, i.e., $\Gamma_s = \Gamma_s(u)$. We aim at driving the shape $\Gamma_s(u)$ (equivalently $\Gamma(u)$) to the desired shape. The main issue is to compute the sensitivity of $J(\Gamma_s(u))$ with respect to u. The equilibrium equation (3.9) becomes $u = -\cos\theta_{cl}$; thus, we must have

$$(4.2) \qquad -1 \leq u \leq 1 \quad \text{on } \Sigma.$$

4.2. Shape derivative of the free boundary PDE. The formulation of the bilevel shape optimization problem is

(4.3)

  minimize $J(\Gamma_s)$

  subject to Γ_s resulting from the solution of (3.10) and $u \in \mathcal{C}^{k+1,\alpha}(\Sigma), |u| \leq 1 - \varrho,$

where $\varrho > 0$ is a small parameter, which is introduced to model the fact that it is usually not possible to drive the contact angle to $0°$ or $180°$. The problem of minimizing $J(\Gamma_s)$ is referred to as the upper-level problem, while the free boundary problem is referred to as the lower-level problem.

Next, thanks to Assumption 3.3 we may introduce the reduced functional

$$\mathcal{J}(u) := J(\Gamma_s(u)).$$

Therefore it is convenient to reformulate the bilevel problem as

(4.4)
$$\begin{aligned} &\text{minimize}\quad \mathcal{J}(u) \\ &\text{subject to } u \in \mathcal{C}^{k+1,\alpha}(\Sigma), |u| \leq 1 - \varrho. \end{aligned}$$

In order to derive optimality conditions we need to compute the derivative of J with respect to Γ_s and the derivative of $\Gamma_s(u)$ with respect to u, in a sense that will be made clear later.

4.2.1. Sensitivity of geometric quantities. In order to compute the derivative of $\mathcal{J}(u)$ with respect to u, we first need some basic shape sensitivity results. Let $D \subset \mathbb{R}^3$ be a fixed box large enough to contain all admissible domains Ω (droplets). Consider a parameterized transformation $T(\mathbf{W}) = I + \mathbf{W}$ associated with a vector field $\mathbf{W} \in \mathcal{C}_b^{k,\alpha}(\mathbb{R}^3, \mathbb{R}^3)$.

In view of (3.10) we need to compute the shape derivative of a few geometric quantities such as $\mathbf{b}_s$ and $\mathbf{b}$. Using the definition $\mathbf{b} := \boldsymbol{\tau} \times \boldsymbol{\nu}$ and a unitary extension of $\mathbf{b}$ to a neighborhood of Σ in the plane $\mathcal{P}$, the $\mathcal{P}$-shape derivative of $\mathbf{b}$ in the direction $\mathbf{W}$ is given by

$$(4.5) \qquad \delta_\Omega^{\mathcal{P}} \mathbf{b}(\mathbf{W}) = \delta_\Omega^{\mathcal{P}} \boldsymbol{\tau}(\mathbf{W}) \times \boldsymbol{\nu} + \boldsymbol{\tau} \times \delta_\Omega^{\mathcal{P}} \boldsymbol{\nu}(\mathbf{W}).$$

According to [30, Chapter 5, formula (5.64)] and choosing a unitary extension of $\mathbf{b}_s$ to a neighborhood of Σ in the plane $\mathcal{P}$, we obtain the $\mathcal{P}$-shape derivatives

$$(4.6) \quad \delta_\Omega^{\mathcal{P}} \boldsymbol{\nu}(\mathbf{W}) = -\nabla_{\mathcal{Q}}(\mathbf{W} \cdot \boldsymbol{\nu}) \text{ and } \delta_\Omega^{\mathcal{P}} \mathbf{b}_s(\mathbf{W}) = -\nabla_{\mathcal{Q}}(\mathbf{W} \cdot \mathbf{b}_s) = -\nabla_\Sigma(\mathbf{W} \cdot \mathbf{b}_s),$$

where $\mathcal{Q}$ is the plane whose normal vector is $\mathbf{b}_s$, $\nabla_{\mathcal{Q}}$ is the tangential gradient on $\mathcal{Q}$, and ∇_Σ is the tangential gradient along Σ. Note that in (4.6) we get the simplification $\delta_\Omega^{\mathcal{P}} \mathbf{b}_s(\mathbf{W}) = -\nabla_\Sigma(\mathbf{W} \cdot \mathbf{b}_s)$ since $\mathbf{b}_s$ lives in the plane $\mathcal{P}$.

Next we compute $\delta_\Omega^{\mathcal{P}} \boldsymbol{\tau}(\mathbf{W})$. Since $\boldsymbol{\tau}$ and $\mathbf{b}_s$ lie in the plane $\mathcal{P}$, we know that $\boldsymbol{\tau} = \mathbf{b}_s^\perp$, where $(b_1, b_2)^\perp = (-b_2, b_1)$ (i.e., a 90° rotation in the plane). Thus,

$$\begin{aligned} \delta_\Omega^{\mathcal{P}} \boldsymbol{\tau}(\mathbf{W}) &= (\delta_\Omega^{\mathcal{P}} \mathbf{b}_s)^\perp = (-\nabla_\Sigma(\mathbf{W} \cdot \mathbf{b}_s))^\perp \\ &= -\boldsymbol{\tau}^\perp \partial_s(\mathbf{W} \cdot \mathbf{b}_s) = \mathbf{b}_s \partial_s(\mathbf{W} \cdot \mathbf{b}_s) \\ &= [\boldsymbol{\tau} \cdot \nabla(\mathbf{W} \cdot \mathbf{b}_s)] \, \mathbf{b}_s, \end{aligned}$$

where $\nabla_\Sigma \equiv \boldsymbol{\tau} \partial_s$ and ∂_s is the derivative with respect to arc-length on Σ and $\boldsymbol{\tau}$ is the unit tangent vector of Σ. Therefore using (4.5) and (4.6) we deduce the following formula:

$$(4.7) \qquad \delta_\Omega^{\mathcal{P}} \mathbf{b}(\mathbf{W}) = [\boldsymbol{\tau} \cdot \nabla(\mathbf{W} \cdot \mathbf{b}_s)]\mathbf{b}_s \times \boldsymbol{\nu} - \boldsymbol{\tau} \times \nabla_{\mathcal{Q}}(\mathbf{W} \cdot \boldsymbol{\nu}).$$

4.2.2. Perturbed weak formulation. Let $\eta : \Sigma \to \mathbb{R}$ and define the following perturbed substrate surface tension (control) on the *fixed* contact line Σ:

$$(4.8) \qquad u_\epsilon = u + \epsilon\eta : \Sigma \to \mathbb{R}.$$

In accordance with (4.4) we assume that $|u_\epsilon| < 1 - \varrho$ for all $\epsilon \in (-1, 1)$.

Remark 4.1. Since $\Gamma = \Gamma(u_\epsilon)$, the perturbation of u *induces a displacement* $\mathbf{W}^* = \mathbf{W}^*(\epsilon) \in \mathcal{V}$ which describes the deformation of $\Gamma(u)$ into $\Gamma(u_\epsilon)$, precisely such that $\Gamma_s(u_\epsilon) = T(\mathbf{W}^*(\epsilon))(\Gamma_s(u))$ and $\Gamma(u_\epsilon) = T(\mathbf{W}^*(\epsilon))(\Gamma(u))$, where $T(\mathbf{W}^*(\epsilon)) := I + \mathbf{W}^*(\epsilon)$. By a formal Taylor expansion, we have $\mathbf{W}^*(\epsilon) = \epsilon(\mathbf{W}^*)'(0) + O(\epsilon^2)$. Thus, $T(\mathbf{W}^*(\epsilon)) \approx I + \epsilon(\mathbf{W}^*)'(0)$. From this, we see that $(\mathbf{W}^*)'(0)$ is simply the instantaneous *perturbation velocity* of Γ.

The existence of such a vector and of a multiplier $p_0(\epsilon)$ is assumed for now and will be proved later in section 4.3. For simplicity we write $\Gamma(u_\epsilon) = \Gamma(\epsilon)$ and similarly for the other sets. For functions, we write $\mathbf{b}_s(\epsilon) := \mathbf{b}_s(\Gamma(\epsilon)) = \mathbf{b}_s((I + \mathbf{W}^*(\epsilon))(\Gamma))$, etc.

Since the control u is defined on Σ, it should "follow" the free boundary $\Sigma(\epsilon) := T(\mathbf{W}^*(\epsilon))(\Sigma)$. Therefore, we define the function

$$(4.9) \qquad \tilde{u}_\epsilon := u_\epsilon \circ T(\mathbf{W}^*(\epsilon))^{-1} : \Sigma(\epsilon) \to \mathbb{R}.$$

We can now consider the following perturbation of the weak formulation (3.10): find $\Omega(\epsilon)$, $\Gamma(\epsilon)$, and $p_0(\epsilon) \in \mathbb{R}$ such that

$$(4.10) \qquad \begin{aligned} \int_{\Sigma(\epsilon)} [\tilde{u}_\epsilon \, \mathbf{b}_s(\epsilon) + \mathbf{b}(\epsilon)] \cdot \mathbf{V} + \int_{\Gamma(\epsilon)} F(\epsilon)\boldsymbol{\nu}(\epsilon) \cdot \mathbf{V} &= 0, \\ \int_{\Omega(\epsilon)} 1 &= C, \end{aligned}$$

for all smooth $\mathbf{V} \in \mathcal{V}$ where

$$F(\epsilon) := \kappa(\epsilon) - G - p_0(\epsilon).$$

In this way we have parameterized the solution $\Gamma(\epsilon)$ in terms of ϵ.

Remark 4.2. The strong form solution of (4.10) (at $\epsilon = 0$) satisfies

$$(4.11) \qquad F(0) = \kappa - G - p_0 = 0 \ \text{ on } \Gamma \quad \text{such that} \quad \int_\Omega 1 = C,$$

$$(4.12) \qquad \cos\theta_{\mathrm{cl}} + u = 0 \ \text{ on } \Sigma.$$

4.2.3. Sensitivity with respect to substrate surface tension. Let $(\cdot)'$ denote the derivative with respect to ϵ at $\epsilon = 0$. Assuming $\mathbf{W}^*(\epsilon)$ is differentiable with respect to ϵ and differentiating the perturbed weak formulation (4.10) with respect to ϵ at $\epsilon = 0$, one obtains an equation for $(\mathbf{W}^*)'(0)$, which is in fact a first-order approximation of $\mathbf{W}^*(\epsilon)$ in a neighborhood of $\epsilon = 0$ since $\mathbf{W}^*(0) \equiv 0$. In the computation of the derivative of the shape functional $\mathcal{J}(u_\epsilon)$ with respect to ϵ at $\epsilon = 0$, one needs only $(\mathbf{W}^*)'(0)$ instead of $\mathbf{W}^*(\epsilon)$; therefore computing $(\mathbf{W}^*)'(0)$ is enough for our purposes. Note that $\mathbf{W}^*(0) = \mathbf{0}$ since $\Gamma(0) = \Gamma$.

Since u and η are defined on the fixed contact line Σ and are *independent* of $\Omega(\epsilon)$, the derivative of u is

$$(4.13) \qquad u' := \frac{d}{d\epsilon} u_\epsilon \bigg|_{\epsilon=0} = \eta.$$

On the other hand $\tilde{u}_\epsilon$ is defined on the moving contact line $\Sigma(\epsilon)$, so that its derivative with respect to ϵ cannot be computed directly. However, we can interpret it as being a $\mathcal{P}$-shape derivative in the direction $(\mathbf{W}^*)'(0)$, i.e., we use definition (2.3) and formally apply the chain rule which yields

$$\frac{d}{d\epsilon} \tilde{u}_\epsilon \bigg|_{\epsilon=0} := \frac{d}{d\epsilon} \tilde{u}_\epsilon \circ T(\mathbf{W}^*(\epsilon)) \bigg|_{\epsilon=0} - \nabla \tilde{u}_{0,E} \cdot (\mathbf{W}^*)'(0)$$

$$(4.14) \qquad\qquad = \frac{d}{d\epsilon} u_\epsilon \bigg|_{\epsilon=0} - \nabla u_{0,E} \cdot (\mathbf{W}^*)'(0) = \eta.$$

We justify (4.14) as follows. First, note that $u_{0,E} = \tilde{u}_{0,E}$ is a unitary extension of u_0 in direction $\mathbf{b}_{\mathrm{s}}$ in the plane $\mathcal{P}$. Without loss of generality, we assume that the tangential component of $\mathbf{W}^*(\epsilon)$ along Σ vanishes, i.e., $\mathbf{W}^*(\epsilon) \cdot \boldsymbol{\tau}(0) = 0$ on Σ. This assumption will be justified later in the proof of Theorem 4.5. Differentiating this formula yields $(\mathbf{W}^*)'(0) \cdot \boldsymbol{\tau}(0) = 0$. Therefore, $(\mathbf{W}^*)'(0)$ is collinear to $\mathbf{b}_{\mathrm{s}}(0)$ due to $\mathbf{W}^*(\epsilon) \cdot \mathbf{e}_z = 0$ (on Σ) for all $\epsilon > 0$. Since $u_{0,E}$ is a unitary extension of u_0 in direction $\mathbf{b}_{\mathrm{s}}$ in the plane $\mathcal{P}$ and $(\mathbf{W}^*)'(0)$ is collinear to $\mathbf{b}_{\mathrm{s}}(0)$, we have $\nabla u_{0,E} \cdot (\mathbf{W}^*)'(0) = 0$, which proves (4.14). We also have $\mathbf{V}' = \mathbf{0}$, i.e., $\mathbf{V}$ is a vector field independent of ϵ.

Now, let us compute the derivative of (4.10) with respect to ϵ using formulas (2.10) and (2.11). Let us introduce the notation for the left-hand side of (4.10):

$$(4.15) \qquad I_1^\epsilon := \int_{\Sigma(\epsilon)} [\tilde{u}_\epsilon \, \mathbf{b}_{\mathrm{s}}(\epsilon) + \mathbf{b}(\epsilon)] \cdot \mathbf{V},$$

$$(4.16) \qquad I_2^\epsilon := \int_{\Gamma(\epsilon)} F(\epsilon) \boldsymbol{\nu}(\epsilon) \cdot \mathbf{V}.$$

Note that the derivative of I_1^ϵ requires the $\mathcal{P}$-*shape derivative*, whereas the derivative of I_2^ϵ requires the *space shape derivative*; see section 2.3. Recall that $\mathbf{b}_s(\epsilon)$ is an abbreviation for $\mathbf{b}_s(\Gamma(\epsilon)) = \mathbf{b}_s((I + \mathbf{W}^*(\epsilon))(\Gamma))$; therefore the derivative of $\mathbf{b}_s(\epsilon)$ in the derivative of I_1^ϵ can be seen as a $\mathcal{P}$-shape derivative, and using the chain rule we obtain

$$\mathbf{b}_s' := \frac{d}{d\epsilon}\mathbf{b}_s(\epsilon)\bigg|_{\epsilon=0} = \frac{d}{d\epsilon}\mathbf{b}_s(I + \mathbf{W}^*(\epsilon)(\Gamma))\bigg|_{\epsilon=0} := \delta_\Omega^{\mathcal{P}}\mathbf{b}_s((\mathbf{W}^*)'(0)),$$

$$\mathbf{b}' := \frac{d}{d\epsilon}\mathbf{b}(\epsilon)\bigg|_{\epsilon=0} = \frac{d}{d\epsilon}\mathbf{b}(I + \mathbf{W}^*(\epsilon)(\Gamma))\bigg|_{\epsilon=0} := \delta_\Omega^{\mathcal{P}}\mathbf{b}((\mathbf{W}^*)'(0)).$$

On the other hand, the derivative of $\boldsymbol{\nu}(\epsilon)$ appearing in the derivative of I_2^ϵ can be seen as a space shape derivative:

$$\boldsymbol{\nu}' := \frac{d}{d\epsilon}\boldsymbol{\nu}(\epsilon)\bigg|_{\epsilon=0} = \frac{d}{d\epsilon}\boldsymbol{\nu}(I + \mathbf{W}^*(\epsilon)(\Gamma))\bigg|_{\epsilon=0} := \delta_\Omega\boldsymbol{\nu}((\mathbf{W}^*)'(0)).$$

Essentially, the derivatives of $I_1^\epsilon, I_2^\epsilon$ are obtained by applying the chain rule and accounting for the induced transformation $T(\mathbf{W}^*(\epsilon))$ of Γ and Σ. For simplicity, let us write $\widehat{\mathbf{W}} := (\mathbf{W}^*)'(0)$. Hence, we get

$$I_1' + I_2' = 0, \qquad \int_\Gamma \widehat{\mathbf{W}} \cdot \boldsymbol{\nu} = 0,$$

where

$$I_1' \overset{(2.11)}{=} \int_\Sigma \mathbf{V} \cdot [u\mathbf{b}_s' + \eta\mathbf{b}_s + \mathbf{b}'] + \kappa_\Sigma(\mathbf{V} \cdot [u\mathbf{b}_s + \mathbf{b}])(\widehat{\mathbf{W}} \cdot \mathbf{b}_s),$$

$$I_2' \overset{(2.9)}{=} \int_\Gamma [F\boldsymbol{\nu} \cdot \mathbf{V}]' + ((\boldsymbol{\nu} \cdot \nabla)[F\boldsymbol{\nu} \cdot \mathbf{V}] + [F\boldsymbol{\nu} \cdot \mathbf{V}]\kappa)(\widehat{\mathbf{W}} \cdot \boldsymbol{\nu}) + \int_\Sigma [F\boldsymbol{\nu} \cdot \mathbf{V}]\,\mathbf{b} \cdot \widehat{\mathbf{W}}.$$

Replacing $\mathbf{b}_s'$ and $\mathbf{b}'$ in I_1' by their corresponding expressions associated with (4.6), (4.7), we get $I_1' = L_0 + L_1 + L_2$,

$$L_0 := \int_\Sigma \eta\mathbf{V} \cdot \mathbf{b}_s,$$

$$L_1 := \int_\Sigma u[-\mathbf{V} \cdot \nabla_\Sigma(\widehat{\mathbf{W}} \cdot \mathbf{b}_s) + \kappa_\Sigma(\mathbf{V} \cdot \mathbf{b}_s)(\widehat{\mathbf{W}} \cdot \mathbf{b}_s)],$$

$$L_2 := \int_\Sigma \mathbf{V} \cdot \{(\boldsymbol{\tau} \cdot \nabla(\widehat{\mathbf{W}} \cdot \mathbf{b}_s))\mathbf{b}_s \times \boldsymbol{\nu} - \boldsymbol{\tau} \times \nabla_{\mathcal{Q}}(\widehat{\mathbf{W}} \cdot \boldsymbol{\nu})\} + \kappa_\Sigma(\mathbf{V} \cdot \mathbf{b})(\widehat{\mathbf{W}} \cdot \mathbf{b}_s).$$

4.2.4. Computation of I_2'. In I_2' we proceed with some simplifications. Due to (4.11), we have $F = 0$ on Γ and Σ. Moreover, $F' = (\kappa - p_0)'$ since $G' = 0$. So, using $F = 0$ and $\mathbf{V}' = 0$, we get

$$I_2' = \int_\Gamma (\kappa - p_0)'\boldsymbol{\nu} \cdot \mathbf{V} + (\boldsymbol{\nu} \cdot \nabla F)(\boldsymbol{\nu} \cdot \mathbf{V})(\widehat{\mathbf{W}} \cdot \boldsymbol{\nu}).$$

Note that unlike G, which is defined in the entire domain Ω, κ is defined only on Γ and can be extended by a constant along the normal $\boldsymbol{\nu}$, so that, since p_0 is a constant, $\boldsymbol{\nu} \cdot \nabla F = \boldsymbol{\nu} \cdot \nabla G$, which yields

$$I_2' = \int_\Gamma (\kappa - p_0)'\boldsymbol{\nu} \cdot \mathbf{V} - (\boldsymbol{\nu} \cdot \nabla G)(\boldsymbol{\nu} \cdot \mathbf{V})(\widehat{\mathbf{W}} \cdot \boldsymbol{\nu}).$$

Continuing, we need to compute the shape derivative $\kappa'(\widehat{\mathbf{W}})$. Considering a unitary extension of $\boldsymbol{\nu}$ constant along $\boldsymbol{\nu}$, the curvature of Γ is given by $\kappa = \nabla \cdot \boldsymbol{\nu}$; see [16, 60]. Therefore, the shape derivative in the direction $\widehat{\mathbf{W}}$ is given by

$$\kappa'(\widehat{\mathbf{W}}) = \nabla \cdot \boldsymbol{\nu}'(\widehat{\mathbf{W}}) = -\nabla \cdot (\nabla_\Gamma(\widehat{\mathbf{W}} \cdot \boldsymbol{\nu})) = -\nabla_\Gamma \cdot \nabla_\Gamma(\widehat{\mathbf{W}} \cdot \boldsymbol{\nu}) = -\Delta_\Gamma(\widehat{\mathbf{W}} \cdot \boldsymbol{\nu}),$$

where Δ_Γ is the Laplace–Beltrami operator.

Now replacing $\kappa'(\widehat{\mathbf{W}})$ in I_2' we get

$$(4.17) \qquad I_2' = \int_\Gamma (-\Delta_\Gamma(\widehat{\mathbf{W}} \cdot \boldsymbol{\nu}) - p_0')\boldsymbol{\nu} \cdot \mathbf{V} - (\boldsymbol{\nu} \cdot \nabla G)(\boldsymbol{\nu} \cdot \mathbf{V})(\widehat{\mathbf{W}} \cdot \boldsymbol{\nu}).$$

Gathering the previous results, we obtain

(4.18)

$$\int_\Sigma \eta \, \mathbf{V} \cdot \mathbf{b}_s + \int_\Sigma u[-\mathbf{V} \cdot \nabla_\Sigma(\widehat{\mathbf{W}} \cdot \mathbf{b}_s) + \kappa_\Sigma(\mathbf{V} \cdot \mathbf{b}_s)(\widehat{\mathbf{W}} \cdot \mathbf{b}_s)]$$

$$+ \int_\Sigma [\mathbf{V} \cdot \{(\boldsymbol{\tau} \cdot \nabla(\widehat{\mathbf{W}} \cdot \mathbf{b}_s))\mathbf{b}_s \times \boldsymbol{\nu} - \boldsymbol{\tau} \times \nabla_\mathcal{Q}(\widehat{\mathbf{W}} \cdot \boldsymbol{\nu})\} + \kappa_\Sigma(\mathbf{V} \cdot \mathbf{b})(\widehat{\mathbf{W}} \cdot \mathbf{b}_s)]$$

$$+ \int_\Gamma (-\Delta_\Gamma(\widehat{\mathbf{W}} \cdot \boldsymbol{\nu}) - \widehat{p}_0)\boldsymbol{\nu} \cdot \mathbf{V} - (\boldsymbol{\nu} \cdot \nabla G)(\boldsymbol{\nu} \cdot \mathbf{V})(\widehat{\mathbf{W}} \cdot \boldsymbol{\nu}) = 0$$

for all $\mathbf{V} \in \mathcal{V}$ and $\int_\Gamma \widehat{\mathbf{W}} \cdot \boldsymbol{\nu} = 0$, where $\widehat{p}_0 := p_0'$ is the Lagrange multiplier for the constant volume constraint.

4.2.5. Strong form PDE for $\widehat{\mathbf{W}} \cdot \boldsymbol{\nu}$. We will now derive a closed set of equations that determine the normal component of $\widehat{\mathbf{W}}$ choosing appropriate test functions in (4.18).

Let $\mathbf{V}$ be such that $\mathbf{V} = \psi\boldsymbol{\nu}$ on Γ, where $\psi : \Gamma \to \mathbb{R}$ is a *compact* function of class $\mathcal{C}^{k,\alpha}$ on Γ, and plug into (4.18). Then all integrals on Σ in (4.18) vanish and this yields

$$(4.19) \qquad \int_\Gamma (-\Delta_\Gamma(\widehat{\mathbf{W}} \cdot \boldsymbol{\nu}) - \widehat{p}_0 - (\boldsymbol{\nu} \cdot \nabla G)(\widehat{\mathbf{W}} \cdot \boldsymbol{\nu}))\psi = 0.$$

This yields the following partial differential equation for $\widehat{\mathbf{W}} \cdot \boldsymbol{\nu}$:

$$(4.20) \qquad -\Delta_\Gamma(\widehat{\mathbf{W}} \cdot \boldsymbol{\nu}) - (\boldsymbol{\nu} \cdot \nabla G)(\widehat{\mathbf{W}} \cdot \boldsymbol{\nu}) - \widehat{p}_0 = 0 \text{ on } \Gamma \quad \text{and} \quad \int_\Gamma \widehat{\mathbf{W}} \cdot \boldsymbol{\nu} = 0.$$

Next, choose $\mathbf{V}$ such that $\mathbf{V} = \psi\mathbf{b}_s$ on Σ with ψ of class $\mathcal{C}^{k,\alpha}$. Note that $\cos\theta_{cl} = \mathbf{b} \cdot \mathbf{b}_s = \boldsymbol{\nu} \cdot \mathbf{e}_z$ and $\sin\theta_{cl} = \boldsymbol{\nu} \cdot \mathbf{b}_s$. Then (4.18) reduces to

$$\int_\Sigma \eta \, \psi + \int_\Sigma u[-\mathbf{b}_s \cdot \nabla_\Sigma(\widehat{\mathbf{W}} \cdot \mathbf{b}_s) + \kappa_\Sigma(\widehat{\mathbf{W}} \cdot \mathbf{b}_s)]\psi$$

$$(4.21) \qquad + \int_\Sigma [\mathbf{b}_s \cdot \{(\boldsymbol{\tau} \cdot \nabla(\widehat{\mathbf{W}} \cdot \mathbf{b}_s))\mathbf{b}_s \times \boldsymbol{\nu} - \boldsymbol{\tau} \times \nabla_\mathcal{Q}(\widehat{\mathbf{W}} \cdot \boldsymbol{\nu})\}$$

$$+ \kappa_\Sigma \cos\theta_{cl}(\widehat{\mathbf{W}} \cdot \mathbf{b}_s)]\psi = 0,$$

where we have used (4.20) to eliminate the last integral in (4.18). Noting that $\mathbf{b}_s \cdot \nabla_\Sigma(\widehat{\mathbf{W}} \cdot \mathbf{b}_s) = 0$ and $\mathbf{b}_s \cdot (\mathbf{b}_s \times \boldsymbol{\nu}) = \boldsymbol{\nu} \cdot (\mathbf{b}_s \times \mathbf{b}_s) = 0$ we get

(4.22)

$$\int_\Sigma \eta\psi + \int_\Sigma u\kappa_\Sigma(\widehat{\mathbf{W}} \cdot \mathbf{b}_s)\psi + \int_\Sigma [-\mathbf{b}_s \cdot [\boldsymbol{\tau} \times \nabla_\mathcal{Q}(\widehat{\mathbf{W}} \cdot \boldsymbol{\nu})] + \kappa_\Sigma \cos\theta_{cl}(\widehat{\mathbf{W}} \cdot \mathbf{b}_s)]\psi = 0.$$

Expanding the surface gradient as $\nabla_{\mathcal{Q}}(\widehat{\mathbf{W}} \cdot \boldsymbol{\nu}) = \boldsymbol{\tau}(\boldsymbol{\tau} \cdot \nabla)(\widehat{\mathbf{W}} \cdot \boldsymbol{\nu}) + \mathbf{e}_z(\mathbf{e}_z \cdot \nabla)(\widehat{\mathbf{W}} \cdot \boldsymbol{\nu})$ we get

$$(4.23) \qquad \begin{aligned} \mathbf{b}_{\mathrm{s}} \cdot [\boldsymbol{\tau} \times \nabla_{\mathcal{Q}}(\widehat{\mathbf{W}} \cdot \boldsymbol{\nu})] &= \mathbf{b}_{\mathrm{s}} \cdot [\boldsymbol{\tau} \times \mathbf{e}_z(\mathbf{e}_z \cdot \nabla)(\widehat{\mathbf{W}} \cdot \boldsymbol{\nu})] \\ &= (\mathbf{b}_{\mathrm{s}} \cdot \mathbf{b}_{\mathrm{s}})(\mathbf{e}_z \cdot \nabla)(\widehat{\mathbf{W}} \cdot \boldsymbol{\nu}) \\ &= (\mathbf{e}_z \cdot \nabla)(\widehat{\mathbf{W}} \cdot \boldsymbol{\nu}) \end{aligned}$$

and

$$(4.24) \quad \widehat{\mathbf{W}} \cdot \boldsymbol{\nu} = (\mathbf{b}_{\mathrm{s}} \cdot \boldsymbol{\nu})(\widehat{\mathbf{W}} \cdot \mathbf{b}_{\mathrm{s}}) + (\boldsymbol{\tau} \cdot \boldsymbol{\nu})(\widehat{\mathbf{W}} \cdot \boldsymbol{\tau}) + (\mathbf{e}_z \cdot \boldsymbol{\nu})(\widehat{\mathbf{W}} \cdot \mathbf{e}_z) = \sin\theta_{\mathrm{cl}} \widehat{\mathbf{W}} \cdot \mathbf{b}_{\mathrm{s}},$$

due to $\widehat{\mathbf{W}} \cdot \mathbf{e}_z = 0$ on Σ and $\boldsymbol{\tau} \cdot \boldsymbol{\nu} = 0$. Plugging (4.24)–(4.24) into (4.22) yields

$$(4.25) \qquad \int_{\Sigma} [\eta - (\mathbf{e}_z \cdot \nabla)(\widehat{\mathbf{W}} \cdot \boldsymbol{\nu})]\psi + \int_{\Sigma} \kappa_{\Sigma} \frac{(u + \cos\theta_{\mathrm{cl}})}{\sin\theta_{\mathrm{cl}}}(\widehat{\mathbf{W}} \cdot \boldsymbol{\nu})\psi = 0.$$

The vector $\mathbf{e}_z$ can be written as

$$\mathbf{e}_z = (\mathbf{b} \cdot \mathbf{e}_z)\mathbf{b} + (\boldsymbol{\nu} \cdot \mathbf{e}_z)\boldsymbol{\nu} = -\sin\theta_{\mathrm{cl}}\mathbf{b} + \cos\theta_{\mathrm{cl}}\boldsymbol{\nu}$$

Also, in view of (4.12), we have $\cos\theta_{\mathrm{cl}} + u = 0$, which gives, plugging in (4.25),

$$\int_{\Sigma} [\eta + \sin\theta_{\mathrm{cl}}(\mathbf{b} \cdot \nabla)(\widehat{\mathbf{W}} \cdot \boldsymbol{\nu}) - \cos\theta_{\mathrm{cl}}(\boldsymbol{\nu} \cdot \nabla)(\widehat{\mathbf{W}} \cdot \boldsymbol{\nu})]\psi = 0 \quad \text{for all smooth } \psi.$$

Finally, assuming $\mathbf{W}^*(\epsilon)$ is constant along the normal $\boldsymbol{\nu}$ (see Theorem 4.5) we get $\cos\theta_{\mathrm{cl}}(\boldsymbol{\nu} \cdot \nabla)(\widehat{\mathbf{W}} \cdot \boldsymbol{\nu}) = 0$. This leads to

$$\int_{\Sigma} [\eta + \sin\theta_{\mathrm{cl}}(\mathbf{b} \cdot \nabla)(\widehat{\mathbf{W}} \cdot \boldsymbol{\nu})]\psi = 0 \quad \text{for all smooth } \psi,$$

which is a Neumann boundary condition. Note that $\mathbf{b} \cdot \nabla = \mathbf{b} \cdot \nabla_{\Gamma}$ since $\mathbf{b}$ is tangent to Γ.

Let us summarize the results. Define $\widehat{W}_{\boldsymbol{\nu}} := \widehat{\mathbf{W}} \cdot \boldsymbol{\nu}$; then $\widehat{W}_{\boldsymbol{\nu}}$ satisfies the following surface PDE:

$$(4.26) \qquad -\Delta_{\Gamma}\widehat{W}_{\boldsymbol{\nu}} - (\boldsymbol{\nu} \cdot \nabla G)\widehat{W}_{\boldsymbol{\nu}} - \widehat{p}_0 = 0 \text{ on } \Gamma \ \text{ such that } \int_{\Gamma} \widehat{W}_{\boldsymbol{\nu}} = 0,$$

$$(4.27) \qquad \mathbf{b} \cdot \nabla_{\Gamma}\widehat{W}_{\boldsymbol{\nu}} = -\frac{\eta}{\sin\theta_{\mathrm{cl}}} \text{ on } \Sigma.$$

Remark 4.3. The well-posedness of (4.26)–(4.27) is crucial for our shape optimization approach. If $G \equiv 0$ and $\widehat{p}_0 \equiv 0$, then it is an elliptic problem with a standard compatibility condition on the Neumann data with the mean value of $\widehat{W}_{\boldsymbol{\nu}}$ set to zero. Indeed, Γ is a known fixed smooth surface, so one can map (4.26)–(4.27) to a flat reference domain. This yields a standard elliptic problem with $\mathcal{C}^{k,\alpha}$ coefficients, for which we know there is a solution [22], [27, Theorem 9.15], [3, Lemma 2.6]; see [19, 47] for more on weak solutions of variable coefficient elliptic problems.

If we include the gravity term G, then one cannot arbitrarily set the mean value of $\widehat{W}_{\boldsymbol{\nu}}$ on Γ. Ergo, we need to enforce $\int_{\Gamma} \widehat{W}_{\boldsymbol{\nu}} = 0$ with the Lagrange multiplier $\widehat{p}_0$. Moreover, the sign of $-(\boldsymbol{\nu} \cdot \nabla G)$ is *indefinite* in general. Therefore, one must invoke the "Fredholm alternative" [22, 27, 42] when studying solutions of (4.26)–(4.27). Note

that if the gravity vector $\mathbf{g}$ points along $-\mathbf{e}_z$ and Γ is convex with $\theta_{\mathrm{cl}} \leq 90°$ (a common situation), then $-(\boldsymbol{\nu} \cdot \nabla G) \geq 0$, so existence and uniqueness follow by the Lax–Milgram lemma [22].

Therefore, in order to make sense of the derivative of the objective functional (see section 4.4), and in view of the previous comments, it is reasonable to make the following assumption.

Assumption 4.4. Suppose Γ is a $\mathcal{C}^{k+1,\alpha}$ surface with boundary Σ of class $\mathcal{C}^{k+1,\alpha}$. The operator $\mathcal{T}$ defined by

$$(4.28) \qquad \mathcal{T} : \mathbb{R} \times \mathcal{C}^{k,\alpha}(\Gamma, \mathbb{R}) \to \mathcal{C}^{k-2,\alpha}(\Gamma, \mathbb{R}) \times \mathcal{C}^{k-1,\alpha}(\Sigma, \mathbb{R}) \times \mathbb{R},$$

$$(4.29) \qquad (\widehat{p}_0, \widehat{W_{\boldsymbol{\nu}}}) \mapsto (f_1, f_2, f_3),$$

where

$$(4.30) \qquad -\Delta_\Gamma \widehat{W_{\boldsymbol{\nu}}} - (\boldsymbol{\nu} \cdot \nabla G)\widehat{W_{\boldsymbol{\nu}}} - \widehat{p}_0 = f_1 \text{ on } \Gamma \text{ such that } \int_\Gamma \widehat{W_{\boldsymbol{\nu}}} = f_3,$$

$$(4.31) \qquad \sin\theta_{\mathrm{cl}}\mathbf{b} \cdot \nabla_\Gamma \widehat{W_{\boldsymbol{\nu}}} = f_2 \text{ on } \Sigma$$

is an isomorphism.

Let us introduce the solution operator A corresponding to (4.26)–(4.27):

$$A : \mathcal{C}^{k-1,\alpha}(\Sigma, \mathbb{R}) \to \mathbb{R} \times \mathcal{C}^{k,\alpha}(\Gamma, \mathbb{R}),$$

$$\eta \mapsto \left(\widehat{p}_0(\eta), \widehat{W_{\boldsymbol{\nu}}}(\eta)\right).$$

In the above, $\widehat{W_{\boldsymbol{\nu}}}$ is defined only on Γ.

4.3. Sensitivity of the free boundary with respect to the substrate surface tension. In the previous section, we have assumed the existence of a flow velocity $\mathbf{W}^*(\epsilon) \in \mathcal{V}$ induced by the perturbation u_ϵ of u which describes the deformation of $\Gamma(u)$ into $\Gamma(u_\epsilon)$, i.e., such that $\Gamma(u_\epsilon) = T(\mathbf{W}^*(\epsilon))(\Gamma(u))$. In this section we prove the existence and differentiability of $\mathbf{W}^*(\epsilon)$ and $p_0(\epsilon)$ for ϵ in a neighborhood of 0 and compute $(\mathbf{W}^*)'(0)$.

For a given vector $\mathbf{W} \in \mathcal{V}$, we define $\Omega_{\mathbf{W}} := T(\mathbf{W})(\Omega)$, $\Gamma_{\mathbf{W}} := T(\mathbf{W})(\Gamma)$, $\Sigma_{\mathbf{W}} := T(\mathbf{W})(\Sigma)$. We denote by $\kappa(\mathbf{W})$ the curvature of $\Gamma_{\mathbf{W}}$ and in a similar way we write $\mathbf{b}(\mathbf{W})$, $\mathbf{b}_{\mathrm{s}}(\mathbf{W})$, $\cos\theta_{\mathrm{cl}}(\mathbf{W}) = \mathbf{b}(\mathbf{W}) \cdot \mathbf{b}_{\mathrm{s}}(\mathbf{W})$ and similarly for the other functions.

THEOREM 4.5. *Let Assumptions 3.3 and 4.4 be satisfied for some given $u \in \mathcal{C}^{k+1,\alpha}(\Sigma, \mathbb{R})$, i.e., we have Γ, Σ are of class $\mathcal{C}^{k+1,\alpha}$. Then there exists an open neighborhood $\mathcal{E}$ of 0 in $\mathbb{R}$ and a function*

$$\mathcal{E} \ni \epsilon \mapsto (p_0^*(\epsilon), \mathbf{W}^*(\epsilon)) \in \mathbb{R} \times \mathcal{V}$$

of class $\mathcal{C}^\infty$ such that

$$\kappa(\mathbf{W}^*(\epsilon)) - G - p_0^*(\epsilon) = 0 \text{ on } \Gamma_{\mathbf{W}^*(\epsilon)} \quad \text{and} \quad \int_{\Omega_{\mathbf{W}^*(\epsilon)}} 1 = C,$$

$$\cos\theta_{\mathrm{cl}}(\mathbf{W}^*(\epsilon)) + \tilde{u}_\epsilon = 0 \text{ on } \Sigma_{\mathbf{W}^*(\epsilon)},$$

and $\mathbf{W}^*(0) = \mathbf{0}$.

Proof. The main tool is to use the implicit function theorem. For $\epsilon \in \mathbb{R}$ and $\eta \in \mathcal{C}^{k+1,\alpha}(\Sigma, \mathbb{R})$ define $u_\epsilon := u + \epsilon\eta$ on Σ and $\tilde{u}_\epsilon := u_\epsilon \circ T(\mathbf{W})^{-1}$ on $\Sigma_{\mathbf{W}}$. For an

arbitrary $\mathbf{W} \in \mathcal{V}$ define the operator $F(p_0, \mathbf{W})$ as the left-hand side of the strong formulation (3.7) on the domain $\Gamma_\mathbf{W}$,

$$F(p_0, \mathbf{W}) := \kappa(\mathbf{W}) - G - p_0 \text{ on } \Gamma_\mathbf{W},$$

and for the left-hand side of (3.9) define

$$B(\epsilon, \mathbf{W}) := \tilde{u}_\epsilon + \cos\theta_{\mathrm{cl}}(\mathbf{W}) \text{ on } \Sigma_\mathbf{W}.$$

Transporting back F and B on the initial sets Γ and Σ using the change of variable $y = T(\mathbf{W})(x) = (I + \mathbf{W})(x)$ yields

(4.32) $$F(p_0, \mathbf{W}) \circ T(\mathbf{W}) := [\kappa(\mathbf{W}) - G] \circ T(\mathbf{W}) - p_0 \text{ on } \Gamma,$$
(4.33) $$B(\epsilon, \mathbf{W}) \circ T(\mathbf{W}) := u_\epsilon + [\cos\theta_{\mathrm{cl}}(\mathbf{W})] \circ T(\mathbf{W}) \text{ on } \Sigma,$$

where we have used the definition $\tilde{u}_\epsilon := u_\epsilon \circ T(\mathbf{W})^{-1}$. For the integral we have

$$\int_{\Omega_\mathbf{W}} 1 = \int_\Omega J_\mathbf{w} \text{ with } J_\mathbf{w} := \det(I + D\mathbf{W}).$$

We introduce the function

$$\Lambda : \mathbb{R} \times \mathbb{R} \times \mathcal{C}^{k,\alpha}(\Gamma, \mathbb{R}) \to \mathcal{C}^{k-2,\alpha}(\Gamma, \mathbb{R}) \times \mathcal{C}^{k-1,\alpha}(\Sigma, \mathbb{R}) \times \mathbb{R}$$
$$(\epsilon, q_0, W_{\boldsymbol{\nu}}) \mapsto \left(F(q_0, \mathbf{W}) \circ T(\mathbf{W}), B(\epsilon, \mathbf{W}) \circ T(\mathbf{W}), \int_\Omega J_{e(W_{\boldsymbol{\nu}})} - C \right),$$

where $W_{\boldsymbol{\nu}}$ is an arbitrary element of $\mathcal{C}^{k,\alpha}(\Gamma, \mathbb{R})$ and e is a linear and continuous extension,

$$e : \mathcal{C}^{k,\alpha}(\Gamma, \mathbb{R}) \to \mathcal{V}.$$

Such an extension exists; indeed the extension from $\mathcal{C}^{k,\alpha}(\Gamma, \mathbb{R})$ to $\mathcal{C}_b^{k,\alpha}(\mathbb{R}^3, \mathbb{R}^3)$ is standard, for instance, by taking $\overline{\mathbf{W}}_1 = W_{\boldsymbol{\nu}}\boldsymbol{\nu}$ on Γ and extending it by a constant along the normal vector. Note that here $\boldsymbol{\nu}$ is indeed of class $\mathcal{C}^{k,\alpha}(\Gamma, \mathbb{R}^3)$ since we have assumed Γ of class $\mathcal{C}^{k+1,\alpha}$. The condition $\mathbf{W} \cdot \mathbf{e}_z = 0$ on $\mathcal{P}$ can be easily obtained by choosing $\mathbf{W} = \overline{\mathbf{W}}_1 + \overline{\mathbf{W}}_2$, where $\overline{\mathbf{W}}_2$ is an appropriate vector field satisfying $\overline{\mathbf{W}}_2 \cdot \boldsymbol{\nu} = 0$ on Γ. Note that since e is linear we have

(4.34) $$D_{W_{\boldsymbol{\nu}}} e(0; \widetilde{W_{\boldsymbol{\nu}}}) = e(\widetilde{W_{\boldsymbol{\nu}}}),$$

where $\widetilde{W_{\boldsymbol{\nu}}}$ denotes an arbitrary element of $\mathcal{C}^{k,\alpha}(\Gamma, \mathbb{R}^3)$. For simplicity we denote $\widetilde{\mathbf{W}} := e(\widetilde{W_{\boldsymbol{\nu}}})$.

Thanks to Assumption 3.3 and since we have assumed that Γ, Σ are of class $\mathcal{C}^{k+1,\alpha}$ we get

$$\Lambda(0, p_0, 0) = (0, 0, 0).$$

In order to apply the implicit function theorem and obtain $\mathbf{W}^*(\epsilon), p_0^*(\epsilon)$, we need to prove that Λ is continuously differentiable and that the Jacobian with respect to the two last variables is an isomorphism. In view of definitions (4.32)–(4.33), the function Λ is $\mathcal{C}^\infty$ with respect to the variable ϵ and q_0. It is also of class $\mathcal{C}^\infty$ with respect to $\mathbf{W}$. Indeed the transported geometric quantities $\kappa(\mathbf{W}) \circ T(\mathbf{W})$, $\boldsymbol{\nu}(\mathbf{W}) \circ T(\mathbf{W})$, $\mathbf{b}(\mathbf{W}) \circ T(\mathbf{W})$, $\mathbf{b}_s(\mathbf{W}) \circ T(\mathbf{W})$, and $\cos\theta_{\mathrm{cl}}(\mathbf{W}) \circ T(\mathbf{W})$ are $\mathcal{C}^\infty$ with respect to $\mathbf{W}$.

We show this property for $\boldsymbol{\nu}(\mathbf{W}) \circ T(\mathbf{W})$ as an example. It is known (see [30, Proposition 5.4.14], for instance) that the vector $\boldsymbol{\nu}(\mathbf{W})$ is obtained by the formula

$$\boldsymbol{\nu}(\mathbf{W}) = \frac{(DT(\mathbf{W})^{-T}\boldsymbol{\nu}) \circ T(\mathbf{W})^{-1}}{\|(DT(\mathbf{W})^{-T}\boldsymbol{\nu})\| \circ T(\mathbf{W})^{-1}} \text{ on } \Gamma_{\mathbf{W}},$$

where $\|\cdot\|$ is the Euclidian norm. Thus we have

$$\boldsymbol{\nu}(\mathbf{W}) \circ T(\mathbf{W}) = \frac{DT(\mathbf{W})^{-T}\boldsymbol{\nu}}{\|(DT(\mathbf{W})^{-T}\boldsymbol{\nu})\|} \text{ on } \Gamma.$$

Next, we have that $DT(\mathbf{W}) = I + D\mathbf{W}$ is linear in $\mathbf{W}$ and writing $DT(\mathbf{W})^{-1} = \sum_{q \geq 0}(-D\mathbf{W})^q$ we see that $DT(\mathbf{W})^{-1}$ is of class $\mathcal{C}^\infty$ with respect to $\mathbf{W}$ for small $\mathbf{W}$. Therefore $\boldsymbol{\nu}(\mathbf{W}) \circ T(\mathbf{W})$ is also of class $\mathcal{C}^\infty$. The determinant $J_{\mathbf{W}} = \det(I + D\mathbf{W})$ is polynomial and continuous for the $\mathcal{C}^\infty$-norm. Since the extension $\mathbf{W} := W_{\boldsymbol{\nu}}\boldsymbol{\nu}$ is linear and continuous, we also get that Λ is of class $\mathcal{C}^\infty$ with respect to $\mathbf{W}$.

Now let us compute the partial derivatives of Λ with respect to q_0 and $W_{\boldsymbol{\nu}}$ at the point $(0, p_0, 0)$ and in the direction $\widetilde{q_0}, \widetilde{W_{\boldsymbol{\nu}}}$. Let Λ_1, Λ_2 denote the two components of Λ. In view of the computations in section 4.2.3 and of (4.26)–(4.27) we obtain

$$D_{q_0, W_{\boldsymbol{\nu}}} \Lambda(0, p_0, 0)(\widetilde{q_0}, \widetilde{W_{\boldsymbol{\nu}}})$$
$$= \left(-\Delta_\Gamma \widetilde{\mathbf{W}} \cdot \boldsymbol{\nu} - (\boldsymbol{\nu} \cdot \nabla G)\widetilde{\mathbf{W}} \cdot \boldsymbol{\nu} - \widetilde{q_0}, \; \sin\theta_{\text{cl}}\mathbf{b} \cdot \nabla_\Gamma \widetilde{\mathbf{W}} \cdot \boldsymbol{\nu}, \; \int_\Gamma \widetilde{\mathbf{W}} \cdot \boldsymbol{\nu}\right).$$

The expression above is independent of the extension e since $\widetilde{\mathbf{W}} \cdot \boldsymbol{\nu} = e(\widetilde{W_{\boldsymbol{\nu}}}) \cdot \boldsymbol{\nu} = \widetilde{W_{\boldsymbol{\nu}}}$ on Γ. We have also used the fact that since e needs to be such that $e(\widetilde{W_{\boldsymbol{\nu}}}) \cdot \mathbf{e}_z = 0$ on $\mathcal{P}$, $\widetilde{\mathbf{W}} \cdot \mathbf{b}_{\text{s}} = e(\widetilde{W_{\boldsymbol{\nu}}}) \cdot \mathbf{b}_{\text{s}}$ can be expressed in terms of $\widetilde{\mathbf{W}} \cdot \boldsymbol{\nu}$ on Σ thanks to $|u| \leq 1 - \rho$ and is therefore independent of the choice of extension e as well.

We observe that $D_{q_0, W_{\boldsymbol{\nu}}} \Lambda(0, p_0, 0)$ is an isomorphism from $\mathbb{R} \times \mathcal{C}^{k,\alpha}(\Gamma, \mathbb{R})$ to $\mathcal{C}^{k-2,\alpha}(\Gamma, \mathbb{R}) \times \mathcal{C}^{k-1,\alpha}(\Sigma, \mathbb{R}) \times \mathbb{R}$ thanks to Assumption 4.4. Thus we may apply the implicit function theorem to Λ, i.e., there exists a neighborhood $\mathcal{E}$ of 0 in $\mathbb{R}$ and a unique $\mathcal{C}^\infty$ function

$$\mathcal{E} \ni \epsilon \mapsto (p_0^*(\epsilon), W_{\boldsymbol{\nu}}^*(\epsilon)) \in \mathbb{R} \times \mathcal{C}^{k,\alpha}(\Gamma, \mathbb{R})$$

such that $\Lambda(\epsilon, p_0^*(\epsilon), W_{\boldsymbol{\nu}}^*(\epsilon)) = (0, 0, 0)$ for all $\epsilon \in \mathcal{E}$ with $W_{\boldsymbol{\nu}}^*(0) = 0$. The statement of the theorem is obtained by defining $\mathbf{W}^*(\epsilon) := e(W_{\boldsymbol{\nu}}^*(\epsilon))$. Obviously, the choice of e is not unique, so $\mathbf{W}^*(\epsilon)$ is not unique either, even if $W_{\boldsymbol{\nu}}^*(\epsilon)$ is. Since the extension e is linear and continuous, we get that

$$\mathcal{E} \ni \epsilon \mapsto (p_0^*(\epsilon), \mathbf{W}^*(\epsilon)) \in \mathbb{R} \times \mathcal{V}$$

is of class $\mathcal{C}^\infty$ by composition, which concludes the proof of the theorem. $\qquad \square$

COROLLARY 4.6. *Let Assumptions 3.3 and 4.4 be satisfied for some given* $u \in \mathcal{C}^{k+1,\alpha}(\Sigma, \mathbb{R})$. *Then the derivative of* $W_{\boldsymbol{\nu}}^*(\epsilon)$ *at* $\epsilon = 0$ *in direction* $\eta \in \mathcal{C}^{k+1,\alpha}(\Sigma, \mathbb{R})$ *is given by*

$$((p_0^*)'(0), (W_{\boldsymbol{\nu}}^*)'(0)) = A(\eta),$$

where A *is the solution operator corresponding to* (4.26)–(4.27). *In addition* $(\mathbf{W}^*)'(0) = e((W_{\boldsymbol{\nu}}^*)'(0))$, *where* e *is the extension from Theorem 4.5.*

Proof. In view of Theorem 4.5 there exists a neighborhood $\mathcal{E}$ of 0 in $\mathbb{R}$ and a unique $\mathcal{C}^\infty$ function

$$\mathcal{E} \ni \epsilon \mapsto (p_0^*(\epsilon), W_{\boldsymbol{\nu}}^*(\epsilon)) \in \mathbb{R} \times \mathcal{C}^{k,\alpha}(\Gamma, \mathbb{R})$$

such that $\Lambda(\epsilon, p_0^*(\epsilon), W_{\boldsymbol{\nu}}^*(\epsilon)) = (0,0,0)$ for all $\epsilon \in \mathcal{E}$ with $W_{\boldsymbol{\nu}}^*(0) = 0$. Differentiating $\Lambda(\epsilon, p_0^*(\epsilon), W_{\boldsymbol{\nu}}^*(\epsilon)) = (0,0,0)$ with respect to ϵ at $\epsilon = 0$ in direction η gives

$$(4.35) \qquad D_\epsilon \Lambda(0, p_0, 0) + D_{q_0, W_{\boldsymbol{\nu}}} \Lambda(0, p_0, 0)(\widehat{p}_0, \widehat{W}_{\boldsymbol{\nu}}) = (0,0,0),$$

where $\widehat{W}_{\boldsymbol{\nu}} := (W_{\boldsymbol{\nu}}^*)'(0)$ and $\widehat{p}_0 := (p_0^*)'(0)$. Since

$$D_\epsilon \Lambda(0, p_0, 0) = (0, \eta, 0)$$

we observe that (4.35) corresponds precisely to (4.26)–(4.27); thus we obtain thanks to Assumption 4.4

$$(\widehat{p}_0, \widehat{W}_{\boldsymbol{\nu}}) = A(\eta).$$

Since $\mathbf{W}^*(\epsilon) = e(W_{\boldsymbol{\nu}}^*(\epsilon))$, we have

$$(\mathbf{W}^*)'(0) = (e(W_{\boldsymbol{\nu}}^*))'(0) = D_{W_{\boldsymbol{\nu}}} e(0; (W_{\boldsymbol{\nu}}^*)'(0)) = e((W_{\boldsymbol{\nu}}^*)'(0)),$$

where we used (4.34). This concludes the proof. $\qquad\square$

4.4. Derivative of the cost functional. Let Σ_d be the target contact line, i.e., the boundary of the target liquid-solid interface Γ_d. Suppose $\phi : \mathcal{P} \to \mathbb{R}$ is a level set function such that

$$\Sigma_d = \{\mathbf{x} \in \mathcal{P} \ : \ \phi(\mathbf{x}) = 0\}$$

and $|\nabla \phi| > 0$ on Σ_d. A typical choice for the level set function is the signed distance to Σ_d. We consider two functionals to optimize:

$$(4.36) \qquad J_1(\Gamma_s) = \int_{\mathcal{P}} \left| \chi_{\{\Gamma_s\}} - \chi_{\{\Gamma_d\}} \right|^2,$$

$$(4.37) \qquad J_2(\Gamma_s) = \frac{1}{2} \int_\Sigma \phi^2, \quad \text{where } \Sigma = \partial \Gamma_s.$$

The functional J_2 is, in a sense, smoother in comparison to J_1 since the indicator functions in J_1 have jumps, whereas the function ϕ is at least continuous. Note the following *reduced* functionals as in (4.4):

$$\mathcal{J}_i(u) := J_i(\Gamma_s(u)), \quad i = 1, 2.$$

Note that in Theorems 4.7 and 4.8 the derivatives of $\mathcal{J}_1$ and $\mathcal{J}_2$ have the same expressions but the adjoint states have different right-hand sides.

THEOREM 4.7 (derivative of $\mathcal{J}_1$). *Let Assumption 3.3 hold, so that we have a unique weak solution to (4.11)–(4.12). Moreover, let Assumption 4.4 hold as well. Then the derivative of $\mathcal{J}_1$ at u, in the direction η, is given by*

$$\mathcal{J}_1'(u; \eta) = -\int_\Sigma \frac{\eta}{\sin \theta_{\text{cl}}} Z_{\boldsymbol{\nu}},$$

where the adjoint states $Z_{\boldsymbol{\nu}}$ and r_0 satisfy

$$(4.38) \qquad -\Delta_\Gamma Z_{\boldsymbol{\nu}} - (\boldsymbol{\nu} \cdot \nabla G) Z_{\boldsymbol{\nu}} - r_0 = 0 \ \ on \ \Gamma \ \ such \ that \ \int_\Gamma Z_{\boldsymbol{\nu}} = 0,$$

$$(4.39) \qquad \mathbf{b} \cdot \nabla_\Gamma Z_{\boldsymbol{\nu}} = \frac{\zeta}{\sin \theta_{\rm cl}} \ \ on \ \Sigma,$$

where $\zeta : \mathcal{P} \to \{-1, 1\}$ is defined by

$$(4.40) \qquad \zeta(\mathbf{x}) := \begin{cases} -1, & \mathbf{x} \in \Gamma_d, \\ 1, & \mathbf{x} \in \Gamma_d^c. \end{cases}$$

Proof. Rewrite $J_1(\Gamma_{\rm s})$ as

$$(4.41) \qquad J_1(\Gamma_{\rm s}) = \int_{\Gamma_{\rm s} \cap \Gamma_d^c} 1 + \int_{\Gamma_{\rm s}^c \cap \Gamma_d} 1 = |\Gamma_{\rm s} \cap \Gamma_d^c| + |\Gamma_{\rm s}^c \cap \Gamma_d|.$$

Therefore, its shape derivative in a direction $\mathbf{V} \in \mathcal{C}_b^{k,\alpha}(\mathbb{R}^3, \mathbb{R}^3)$ is

$$(4.42) \qquad \delta_{\Gamma_{\rm s}} J_1(\Gamma_{\rm s}; \mathbf{V}) = \int_{\Sigma \cap \Gamma_d^c} \mathbf{V} \cdot \mathbf{b}_{\rm s} - \int_{\Sigma \cap \Gamma_d} \mathbf{V} \cdot \mathbf{b}_{\rm s} = \int_\Sigma \zeta \mathbf{V} \cdot \mathbf{b}_{\rm s}.$$

Since $\mathcal{J}_1(u_\epsilon) = J_1((I + \mathbf{W}^*(\epsilon))(\Gamma_{\rm s}(u)))$ we may apply the chain rule thanks to Theorem 4.5. So, by (4.42), the derivative of $\mathcal{J}_1(u)$ is

$$\mathcal{J}_1'(u; \eta) = \delta_{\Gamma_{\rm s}} J_1(\Gamma_{\rm s}(u), (\mathbf{W}^*)'(0)),$$

where $\mathbf{W}^*(\epsilon)$ is given by Theorem 4.5. Thus, using (4.24) and $\widehat{W}_{\boldsymbol{\nu}} := (\mathbf{W}^*)'(0) \cdot \boldsymbol{\nu}$, we obtain

$$\mathcal{J}_1'(u; \eta) = \delta_{\Gamma_{\rm s}} J_1(\Gamma_{\rm s}(u), (\mathbf{W}^*)'(0)) = \int_\Sigma \zeta \, (\mathbf{W}^*)'(0) \cdot \mathbf{b}_{\rm s} = \int_\Sigma \frac{\zeta}{\sin \theta_{\rm cl}} \widehat{W}_{\boldsymbol{\nu}}.$$

Standard arguments show that

$$\int_\Sigma \frac{\zeta}{\sin \theta_{\rm cl}} \widehat{W}_{\boldsymbol{\nu}} = \int_\Sigma (\mathbf{b} \cdot \nabla_\Gamma Z_{\boldsymbol{\nu}}) \widehat{W}_{\boldsymbol{\nu}} = \int_\Sigma (\mathbf{b} \cdot \nabla_\Gamma \widehat{W}_{\boldsymbol{\nu}}) Z_{\boldsymbol{\nu}} = -\int_\Sigma \frac{\eta}{\sin \theta_{\rm cl}} Z_{\boldsymbol{\nu}}. \qquad \square$$

THEOREM 4.8 (derivative of $\mathcal{J}_2$). *Let Assumption 3.3 hold, so that we have a unique weak solution to (4.11)–(4.12). Moreover, let Assumption 4.4 hold as well. Then the derivative of $\mathcal{J}_2$ at u, in the direction η, is given by*

$$\mathcal{J}_2'(u; \eta) = -\int_\Sigma \frac{\eta}{\sin \theta_{\rm cl}} Z_{\boldsymbol{\nu}},$$

where the adjoint states $Z_{\boldsymbol{\nu}}$ and r_0 satisfy

$$(4.43) \qquad -\Delta_\Gamma Z_{\boldsymbol{\nu}} - (\boldsymbol{\nu} \cdot \nabla G) Z_{\boldsymbol{\nu}} - r_0 = 0 \ \ on \ \Gamma \ \ such \ that \ \int_\Gamma Z_{\boldsymbol{\nu}} = 0,$$

$$(4.44) \qquad \mathbf{b} \cdot \nabla_\Gamma Z_{\boldsymbol{\nu}} = \frac{1}{2 \sin \theta_{\rm cl}} [(\mathbf{b}_{\rm s} \cdot \nabla) \phi^2 + \kappa_\Sigma \phi^2] \ \ on \ \Sigma.$$

Proof. We use similar notation as in the proof of Theorem 4.7. We apply a standard shape derivative formula to J_2:

$$(4.45) \qquad \delta J_2(\Gamma_{\rm s}; \mathbf{V}) = \frac{1}{2} \int_\Sigma [(\mathbf{b}_{\rm s} \cdot \nabla) \phi^2 + \kappa_\Sigma \phi^2](\mathbf{V} \cdot \mathbf{b}_{\rm s}),$$

which, with (4.24), yields

$$\mathcal{J}_2'(u;\eta) = \delta_{\Gamma_{\mathrm{s}}} J_2(\Gamma_{\mathrm{s}}(u), (\mathbf{W}^*)'(0)) = \int_\Sigma \frac{1}{2\sin\theta_{\mathrm{cl}}} [(\mathbf{b}_{\mathrm{s}} \cdot \nabla)\phi^2 + \kappa_\Sigma \phi^2] \widehat{W}_{\boldsymbol{\nu}}.$$

Using the adjoint equations, we obtain

$$\int_\Sigma \frac{1}{2\sin\theta_{\mathrm{cl}}} [(\mathbf{b}_{\mathrm{s}} \cdot \nabla)\phi^2 + \kappa_\Sigma \phi^2] \widehat{W}_{\boldsymbol{\nu}} = \int_\Sigma (\mathbf{b} \cdot \nabla_\Gamma Z_{\boldsymbol{\nu}}) \widehat{W}_{\boldsymbol{\nu}}$$
$$= \int_\Sigma (\mathbf{b} \cdot \nabla_\Gamma \widehat{W}_{\boldsymbol{\nu}}) Z_{\boldsymbol{\nu}} = -\int_\Sigma \frac{\eta}{\sin\theta_{\mathrm{cl}}} Z_{\boldsymbol{\nu}},$$

which gives the assertion. ☐

5. Numerical results. We describe our shape optimization algorithm and present numerical results. First, we explain our handling of the control function u where we only consider its restriction to Σ (not on the whole substrate). Then we describe the different steps of the numerical algorithm. For the lower-level problem (the free boundary problem), an L^2 gradient flow and a semi-implicit approach for the discretization are used. For the upper-level problem (the control problem), we use a gradient descent method where the descent direction is found using an appropriate regularization on Σ.

5.1. Optimization algorithm.

5.1.1. Interpretation and handling of the control. Recall that the control corresponds to a difference of substrate surface tensions on the contact line, i.e., $u = (\gamma_{\mathrm{s}} - \gamma_{\mathrm{s,g}})|_\Sigma$. Moreover, the cost functional sensitivities (at the current equilibrium contact line Σ) *only depend* on u and η defined on Σ (see Theorems 4.7 and 4.8), so any gradient-based optimization method can only make *local updates* to u *on* Σ. Thus, given an equilibrium shape Σ with associated control u, we compute a descent perturbation $\hat{\eta} : \Sigma \to \mathbb{R}$ which is *only* defined on Σ.

Keeping Σ fixed, it is clear how to update u on Σ, say, for performing a line search. However, one must then solve the "forward" problem, i.e., find a *new* equilibrium solution of (3.10) for the *new* control. This will certainly require the contact line to change position, which is problematic since the new control is only defined on the previously known Σ. Therefore, the new control is defined in a Lagrangian way when computing the corresponding solution of (3.10). See Remark 5.2 in section 5.3.

Of course, this is not practical for a real system. In fact, because there is a bijective map between u and θ_{cl} (i.e., $u = -\cos(\theta_{\mathrm{cl}})$ with $0 \leq \theta_{\mathrm{cl}} \leq \pi$), we are really controlling the *local* contact angle of the droplet. Effectively, this means that θ_{cl} is set to a fixed value at each *material* point of Σ when computing the equilibrium solution of (3.10). There is some justification for this in the context of electrowetting [12, 23, 40, 72, 73, 74, 77]. In this case, it is well known that one can control the local contact angle by applying an electric field to the droplet [50]. Of course, the "resolution" of the control is limited by the electrode grid size.

5.1.2. Descent directions. In section 4.4, we computed the derivatives $\mathcal{J}_i'(u;\eta)$, $i = 1, 2$. We would like to obtain a smooth descent direction $\hat{\eta}$, i.e., such that

$$\mathcal{J}_i'(u;\hat{\eta}) < 0.$$

To find it, we can look for a solution $\hat{\eta} \in \mathbb{B}_\Sigma$ such that

(5.1) $$b_\Sigma(\hat{\eta}, v) = -\mathcal{J}_i'(u;v) \text{ for all } v \in \mathbb{B}_\Sigma,$$

where $\mathbb{B}_\Sigma$ is an appropriate function space and $b_\Sigma : \mathbb{B}_\Sigma \times \mathbb{B}_\Sigma \to \mathbb{R}$ is a symmetric positive definite bilinear form. The solution $\hat{\eta}$ is indeed a descent direction since

$$\mathcal{J}_i'(u;\hat{\eta}) = -b_\Sigma(\hat{\eta},\hat{\eta}) < 0.$$

Examples are

$$(5.2) \qquad \mathbb{B}_\Sigma = L^2(\Sigma) \quad \text{and} \quad b_\Sigma(w,v) = \int_\Sigma w\,v,$$

$$\mathbb{B}_\Sigma = H^1(\Sigma) \quad \text{and} \quad b_\Sigma(w,v) = \int_\Sigma w\,v + \int_\Sigma \nabla_\Sigma w \cdot \nabla_\Sigma v.$$

Examples of this approach can be found in [10, 17, 43, 71, 75].

In our results, we use the second line of (5.2). Furthermore, Σ is discretized by a piecewise linear polygonal curve Σ_h (see section 5.2.3), and we replace $\mathbb{B}_\Sigma$ by $\mathbb{B}_{\Sigma_h}$, the space of continuous piecewise linear functions defined on Σ_h, which conforms to $H^1(\Sigma_h)$. Hence, u and $\hat{\eta}$ are functions in $\mathbb{B}_{\Sigma_h}$ with nodal values defined on the vertices (corners) of Σ_h.

5.1.3. Gradient descent. In order to find a descent direction $\hat{\eta}$, we must first have a solution of the geometrically nonlinear system (3.10) (i.e., the free boundary problem or lower-level problem). This is computed by a gradient flow scheme (see section 5.2). Then, we must solve the adjoint problem to obtain $\mathcal{J}_i'$, followed by the descent direction solve (5.1). Next, we update u using a standard backtracking line search. The process repeats with the solution of (3.10) again and is iterated until some convergence criterion is satisfied. We stopped once the difference in the cost functional, between consecutive iterations of the optimization, was sufficiently small. Section 5.3 gives further details on the algorithm.

The inequality constraint on u should also be enforced. This is a standard "box constraint," for which a simple projection scheme works well [33, 35, 65]. In our numerical examples in section 5.4, this constraint was never active.

5.2. L^2 gradient flow. In order to solve the lower-level problem, i.e., to compute equilibrium droplet shapes with variable substrate surface tension in (3.10), we use a gradient flow variational method described as follows.

5.2.1. Weak formulation. Rewriting (3.10), we get

$$\delta_\Omega \mathcal{L}(\Omega, p_0; \mathbf{V}) = \int_\Sigma u\,\mathbf{b}_{\mathrm{s}} \cdot \mathbf{V} + \int_\Gamma \nabla_\Gamma \cdot \mathbf{V} - \int_\Gamma G\boldsymbol{\nu} \cdot \mathbf{V} - p_0 \int_\Gamma \boldsymbol{\nu} \cdot \mathbf{V}$$

$$(5.3) \qquad = \int_\Sigma u\,\mathbf{b}_{\mathrm{s}} \cdot \mathbf{V} + \int_\Gamma \nabla_\Gamma(\mathbf{X} \circ \mathbf{X}^{-1}) : \nabla_\Gamma \mathbf{V} - \int_\Gamma G\boldsymbol{\nu} \cdot \mathbf{V} - p_0 \int_\Gamma \boldsymbol{\nu} \cdot \mathbf{V},$$

where $\mathrm{id}_\Gamma = \mathbf{X} \circ \mathbf{X}^{-1}$ and $\mathbf{X}(t) : \mathcal{M} \to \Gamma(t)$ is a parameterization of $\Gamma \equiv \Gamma(t)$ in terms of a reference manifold $\mathcal{M}$. Applying the L^2 gradient flow methodology, we want to find $\mathbf{X}(t)$ in $\mathbb{V}(\mathcal{M})$ such that

$$\int_{\Gamma(t)} (\partial_t \mathbf{X} \circ \mathbf{X}^{-1} \cdot \boldsymbol{\nu})(\mathbf{V} \cdot \boldsymbol{\nu}) = -\delta_\Omega \mathcal{L}(\Omega, p_0; \mathbf{V}) \quad \text{for all } \mathbf{V} \text{ in } \mathbb{V}(\mathcal{M}),$$

$$(5.4) \qquad \int_{\Gamma(t)} \partial_t \mathbf{X} \circ \mathbf{X}^{-1} \cdot \boldsymbol{\nu} = 0,$$

where $\partial\mathcal{M}$ is contained in the plane $\{z = 0\}$ and

$$(5.5) \qquad \mathbb{V}(\mathcal{M}) = \{\mathbf{V} \in H^1(\mathcal{M}) : \mathbf{V} \cdot \mathbf{e}_z = 0, \text{ on } \partial\mathcal{M}\}.$$

5.2.2. Semi-implicit method. We use a semi-implicit approach to discretize the gradient flow in time. Thus, at each pseudo-time-step, we solve the following problem. Find $\mathbf{V}^{n+1}$, $\mathbf{X}^{n+1}$ (at time t_{n+1}) in $\mathbb{V}$, p_0 in $\mathbb{R}$, such that

$$
\int_\Gamma (\mathbf{V}^{n+1} \cdot \boldsymbol{\nu})(\mathbf{Y} \cdot \boldsymbol{\nu}) = -\int_\Sigma u\, \mathbf{b}_{\mathrm{s}} \cdot \mathbf{Y} - \int_\Gamma \nabla_\Gamma \mathbf{X}^{n+1} : \nabla_\Gamma \mathbf{Y}
$$

(5.6)
$$
+ \int_\Gamma G\boldsymbol{\nu} \cdot \mathbf{Y} + p_0 \int_\Gamma \mathbf{Y} \cdot \boldsymbol{\nu} \quad \text{for all } \mathbf{Y} \text{ in } \mathbb{V},
$$

$$
\mathbf{X}^{n+1} = \mathbf{X}^n + \delta t \mathbf{V}^{n+1}, \qquad \int_\Gamma \mathbf{V}^{n+1} \cdot \boldsymbol{\nu} = 0,
$$

where $\Gamma \equiv \Gamma^n$ is the current (known) domain at time t_n, and we have made the following identifications to simplify notation: $\mathbf{X}^{n+1} \equiv \mathbf{X}^{n+1} \circ (\mathbf{X}^n)^{-1}$, $\mathbf{V}^{n+1} \equiv \mathbf{V}^{n+1} \circ (\mathbf{X}^n)^{-1}$, $\mathbf{Y} \equiv \mathbf{Y} \circ (\mathbf{X}^n)^{-1}$. Combining the update equation for $\mathbf{X}$ with the weak formulation, we obtain a weak formulation for $\mathbf{V}^{n+1}$ and p_0 only, i.e., find $\mathbf{V}^{n+1}$ in $\mathbb{V}$, p_0 in $\mathbb{R}$, and $\mathbf{X}^{n+1}$ in $\mathbb{V}$ such that

(5.7)
$$
a^n(\mathbf{V}^{n+1}, \mathbf{Y}) + b^n(p_0, \mathbf{Y}) = F^n(\mathbf{Y}) \quad \text{for all } \mathbf{Y} \text{ in } \mathbb{V},
$$
$$
b^n(r, \mathbf{V}^{n+1}) = 0 \quad \text{for all } r \text{ in } \mathbb{R},
$$
$$
\mathbf{X}^{n+1} = \mathbf{X}^n + \delta t \mathbf{V}^{n+1},
$$

where the forms are defined as

(5.8)
$$
a^n(\mathbf{V}, \mathbf{Y}) = \int_{\Gamma^n} (\mathbf{V} \cdot \boldsymbol{\nu}^n)(\mathbf{Y} \cdot \boldsymbol{\nu}^n) + \delta t \int_{\Gamma^n} \nabla_{\Gamma^n} \mathbf{V} : \nabla_{\Gamma^n} \mathbf{Y},
$$
$$
b^n(r, \mathbf{Y}) = -r \int_{\Gamma^n} \mathbf{Y} \cdot \boldsymbol{\nu}^n,
$$
$$
F^n(\mathbf{Y}) = -\int_{\Gamma^n} \nabla_{\Gamma^n} \cdot \mathbf{Y} - \int_{\Sigma^n} u^n\, \mathbf{b}_{\mathrm{s}}^n \cdot \mathbf{Y} + \int_{\Gamma^n} G\mathbf{Y} \cdot \boldsymbol{\nu}^n,
$$

and we have noted the explicit dependence on the time-step n. Note that $\mathbf{X}^n$ is the parameterization of Γ^n and Σ^n, and $\mathbf{X}^{n+1}$ is computed after solving for $\mathbf{V}^{n+1}$. Hence, starting from an initial shape Γ^0 and control u^0, we generate sequences $\{\Gamma^n\}$ and $\{u^n\}$ by repeatedly solving (5.7) until we reach an equilibrium solution. In practice, we stop this iterative procedure once $\|\mathbf{X}^{n+1} - \mathbf{X}^n\|_{L^\infty}$ is sufficiently small.

Running this iterative procedure requires us to transport the control u as Σ evolves along the pseudo-time of the gradient flow (similar to (4.9)). In other words, given u^n on Σ^n (at the nth time-step), we solve (5.7) to obtain $\mathbf{X}^{n+1}$ (and Σ^{n+1}) and define

(5.9)
$$
u^{n+1} = u^n \circ \mathbf{X}^n \circ (\mathbf{X}^{n+1})^{-1} \quad \text{on } \Sigma^{n+1}.
$$

5.2.3. Finite elements. In our computations, we represent Γ by an unstructured mesh. To this end, we replace Γ by a triangulated surface Γ_h and replace $\mathbb{V}$ by $\mathbb{V}_h \subset \mathbb{V}$, which is a conforming finite element space of continuous piecewise linear "hat" functions on Γ_h. See [5, 6, 7, 18, 24, 69] for examples of this methodology.

The contact line is represented by Σ_h, i.e., the boundary of Γ_h, which is a polygonal curve in the plane $\mathcal{P}$. Furthermore, the discrete control, u_h, is represented by a continuous piecewise linear function defined on Σ_h (recall $\mathbb{B}_{\Sigma_h}$ in section 5.1.2). In this setting, it is easy to implement (5.9). Since the mesh topology does not change

during one time-step, one can simply keep the nodal values of u_h fixed during one time-step. This exactly captures (5.9).

Remark 5.1. This type of numerical method is commonly called a front-tracking approach, because the interface Γ is explicitly tracked. These methods sometimes exhibit mesh distortion, which can lead to re-meshing (change of mesh topology) [53]. In this case, u_h must be transferred (or interpolated) from one mesh to another. There are different ways to accomplish this. For the numerical examples we present, no re-meshing was necessary. For simplicity of notation, we drop the h subscript in the following sections.

5.3. Algorithm. The previous sections are summarized in Algorithm 1. Note that in the inner **while** loop, we must solve the discrete forward problem (5.7) (to equilibrium) for each test control u_{test}. The adjoint problem is solved by a finite element method, similar to what is described in section 5.2.3.

ALGORITHM 1. DROPLET CONTROL: SOLVE THE BILEVEL OPTIMIZATION PROBLEM

Input: The target contact line Σ_d and an initialization of the control u_0.
Backtracking coefficient $0 < c < 1$; default: $c = 1/2$. Cost tolerance
tol; default $10^{-5} \leq tol \leq 10^{-7}$. Minimum step size: $\alpha_{tol} = 10^{-5}$.
Output: The optimal control u and the corresponding droplet's contact line
$\Sigma(u)$.

1   $u \leftarrow u_0$;
2   STOP $\leftarrow$ false;
3   Determine $\Sigma(u)$ by solving the lower level problem (i.e., solve the discrete free boundary problem (5.7) to equilibrium).;
4   **while** *not* STOP **do**
5   Compute the discrete adjoint state $Z_{\boldsymbol{\nu}}, r_0$ using (4.38)–(4.39) or (4.43)–(4.44).;
6   Compute the derivative $\mathcal{J}_i'(u; \eta)$ and find a descent direction $\hat{\eta}$ using the method described in section 5.1.2.;
7     $\alpha \leftarrow 1.0$;
8     $u_{\text{test}} \leftarrow u + \alpha\hat{\eta}$ (Obtain $\Sigma(u_{\text{test}})$ through (5.7).);
9   **while** $\mathcal{J}_i(u_{\text{test}}) \geq \mathcal{J}_i(u)$ and $\alpha \geq \alpha_{tol}$ **do**
10       $\alpha \leftarrow \alpha * c$;
11       $u_{\text{test}} \leftarrow u + \alpha\hat{\eta}$ (Obtain $\Sigma(u_{\text{test}})$ through (5.7).);
12   **if** $|\mathcal{J}_i(u) - \mathcal{J}_i(u_{\text{test}})| < tol$ or $\alpha < \alpha_{tol}$ **then**
13   STOP $\leftarrow$ true;
14     $u \leftarrow u_{\text{test}}$ (Note: we also have $\Sigma(u)$.);
15   **return** u *and* $\Sigma(u)$.;

Remark 5.2. Algorithm 1 generates a sequence of contact lines $\{\Sigma^k\}$ and controls $\{u^k\}$. So it seems there should be a Lagrangian update of u^k as described in (4.9). This is automatically accomplished by (5.9) when solving the forward problem (5.7) to equilibrium.

5.4. Optimization results. Algorithm 1 was implemented in MATLAB using the FELICITY toolbox [66]. The following sections show some examples of our computational method. Specifically, we consider the following desired footprint shapes:
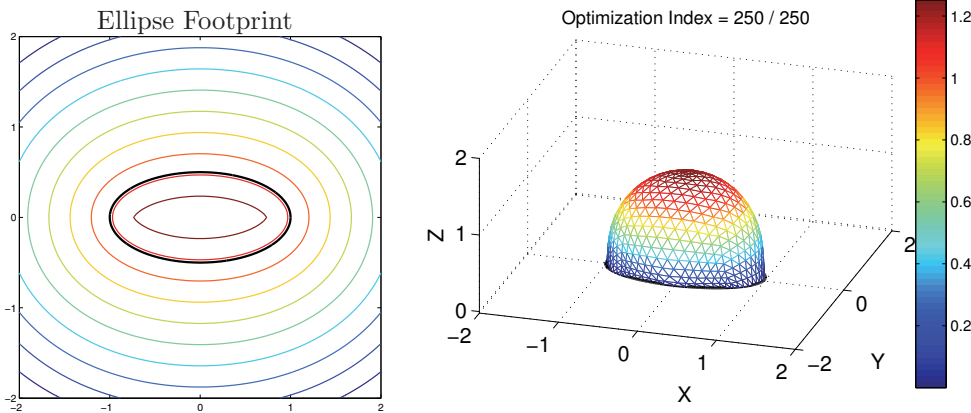
FIG. 2. *Left: Desired footprint shape Σ_d (thick black curve) plotted in the plane $\mathcal{P}$. The colored contours are level sets of ϕ. Right: the optimal droplet shape Γ after the optimization method converges.*
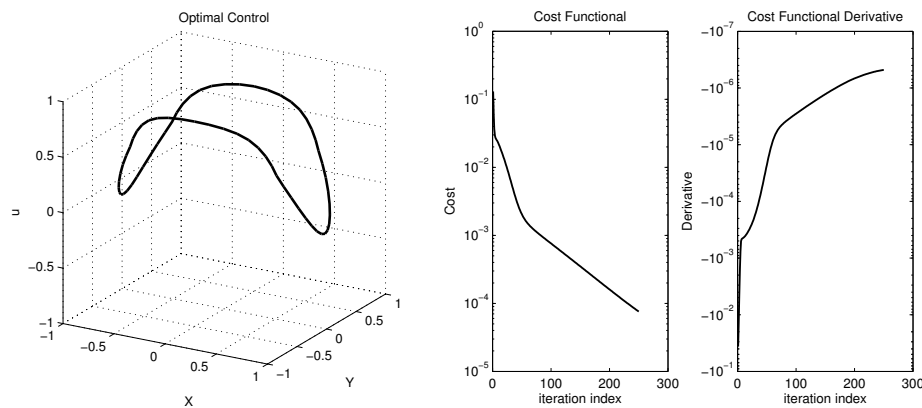

FIG. 3. *Left: Optimal control function u for the desired footprint Σ_d in Figure 2. Right: Optimization history for the objective functional (4.37) and directional derivative (recall Theorem 4.8). The initial value of $\mathcal{J}_2$ is 0.1306 and the final value is 7.6×10^{-5}.*

ellipse, square, and four-leaf clover. The results presented here are obtained using the functional $\mathcal{J}_2$.

5.4.1. Ellipse footprint. We take Σ_d to be an ellipse with associated distance function ϕ; recall (4.37). See Figures 2 and 3 for plots of the desired footprint Σ_d, optimal droplet shape Γ, optimal control u, and optimization history. In this case, we can easily obtain the desired footprint.

5.4.2. Square footprint. We take Σ_d to be a square with associated distance function ϕ; recall (4.37). See Figures 4 and 5 for plots of the desired footprint Σ_d, optimal droplet shape Γ, optimal control u, and optimization history. As the optimization progresses, the droplet's contact line Σ asymptotically approaches the corners of the square.

5.4.3. Four-leaf clover footprint. We take Σ_d to be a four-leaf clover with associated distance function ϕ; recall (4.37). See Figures 6 and 7 for plots of the
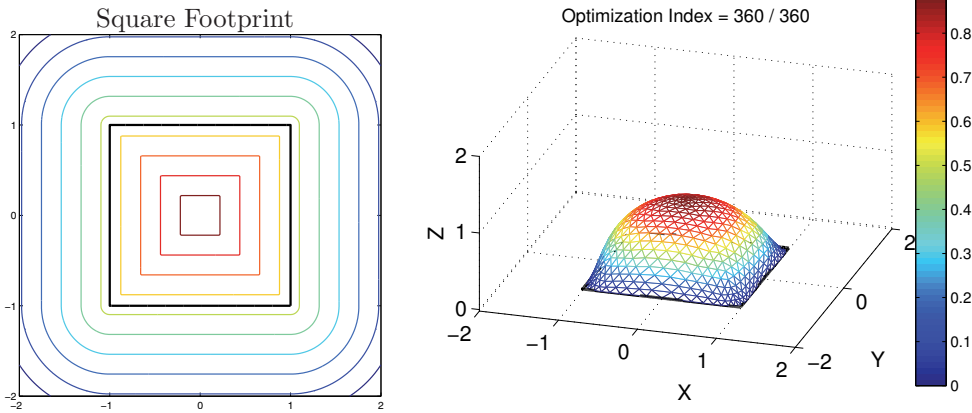
FIG. 4. *Left: Desired footprint shape* Σ_d *(thick black curve) plotted in the plane* $\mathcal{P}$. *The colored contours are level sets of* ϕ. *Right: the optimal droplet shape* Γ *after the optimization method converges.*
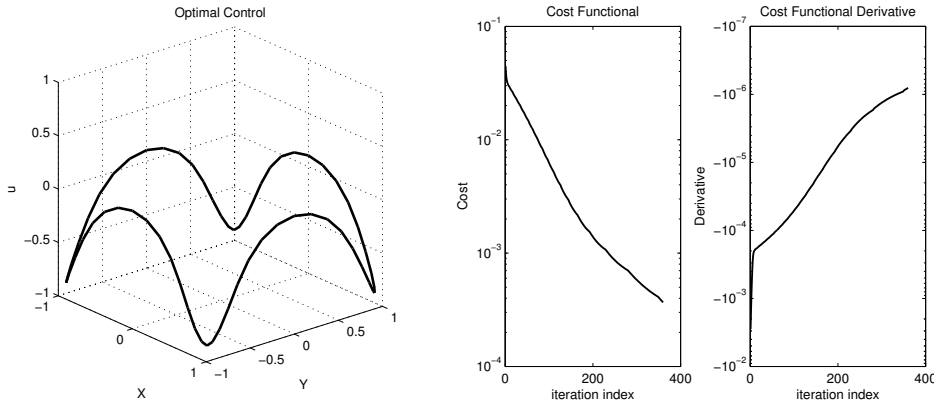

FIG. 5. *Left: Optimal control function* u *for the desired footprint* Σ_d *in Figure* 4. *Right: Optimization history for the objective functional* (4.37) *and directional derivative (recall Theorem* 4.8*). The initial value of* $\mathcal{J}_2$ *is* 4.47×10^{-2} *and the final value is* 3.7×10^{-4}.

desired footprint Σ_d, optimal droplet shape Γ, optimal control u, and optimization history. Almost the full range of the control u (between -1 and $+1$) is utilized here to obtain the clover shape.

5.5. Summary. In this paper, we have studied the controllability of the footprint of a sessile droplet sitting on a surface via substrate surface tension. This amounts to the control of a free boundary, which can also be seen as a bilevel shape optimization problem. We have performed the rigorous sensitivity analysis of the free boundary with respect to the substrate surface tension. We have shown that a small variation of the substrate surface tension leads to a perturbation of the free boundary which can be described by a vector field solution of an elliptic PDE on the surface of the droplet. Thanks to these results, we were able to devise a numerical algorithm to solve the free boundary problem at the lower level and to control the free boundary effectively at the upper level of the optimization.

The numerical results show that we can compute the variable substrate surface tension coefficient that will drive the liquid-solid interface (i.e., the footprint) to a
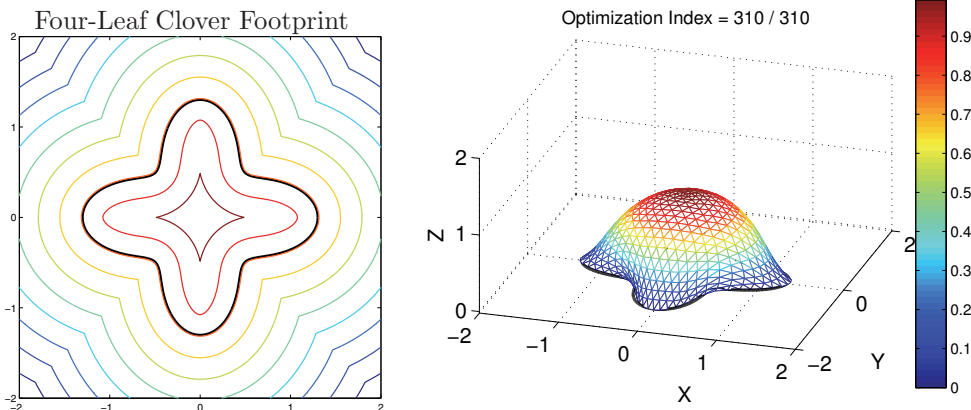
Fig. 6. *Left: Desired footprint shape Σ_d (thick black curve) plotted in the plane $\mathcal{P}$. The colored contours are level sets of ϕ. Right: the optimal droplet shape Γ after the optimization method converges.*
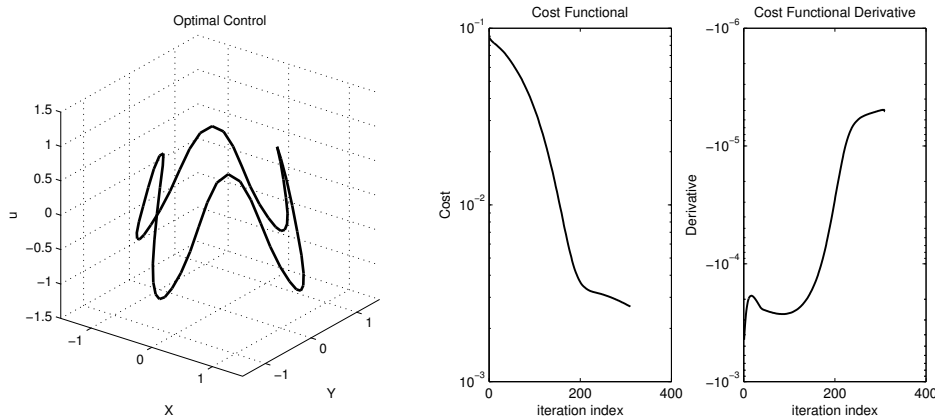

Fig. 7. *Left: Optimal control function u for the desired footprint Σ_d in Figure 6. Right: Optimization history for the objective functional (4.37) and directional derivative (recall the Theorem 4.8). The initial value of $\mathcal{J}_2$ is 8.84×10^{-2} and the final value is 2.7×10^{-3}.*

reasonable desired shape. Characterizing the limits on the types of shapes that are achievable is an interesting, and difficult, area to explore. Another possible extension is to optimize the full surface tension coefficient in the plane of the substrate, instead of merely controlling the contact angle (recall the discussion in section 5.1.1). This is significantly more challenging because the problem becomes time-dependent since one must track the evolution of the droplet. In this case, the goal would be to design a static surface tension field for the substrate such that if a droplet is deposited onto any part of the solid, then it will migrate toward a desired location with a desired footprint.

We can also modify the problem to be more relevant to applications. For instance, an electrostatic field may be added which changes the control to be the applied boundary voltage (i.e., electrowetting; see [70, 73, 74]). Here, an additional PDE constraint comes into play (e.g., Poisson's equation in three dimensions). One can also add inequality constraints for the geometry of the contact line Σ.

　
REFERENCES

[1] A. Alarcon and R. Souam, *Capillary Surfaces Inside Polyhedral Regions*, arXiv:1401.6935, 2014.

[2] H. W. Alt, *Verzweigungspunkte von H-Flächen.* I, Math. Z., 127 (1972), pp. 333–362.

[3] H. Antil and S. W. Walker, *Optimal control of surface shape*, submitted.

[4] G. Azimi, R. Dhiman, H.-M. Kwon, A. T. Paxson, and K. K. Varanasi, *Hydrophobicity of rare-earth oxide ceramics*, Nature Materials, 12 (2013), pp. 315–320.

[5] E. Bänsch, *Finite element discretization of the Navier-Stokes equations with a free capillary surface*, Numer. Math., 88 (2001), pp. 203–235.

[6] E. Bänsch, P. Morin, and R. H. Nochetto, *A finite element method for surface diffusion: The parametric case*, J. Comput. Phys., 203 (2005), pp. 321–343.

[7] J. W. Barrett, H. Garcke, and R. Nürnberg, *Parametric approximation of Willmore flow and related geometric evolution equations*, SIAM J. Sci. Comput., 31 (2008), pp. 225–253.

[8] T. J. Battin, W. T. Sloan, S. Kjelleberg, H. Daims, I. M. Head, T. P. Curtis, and L. Eberl, *Microbial landscapes: New paths to biofilm research*, Nature Rev. Microbiol., 5 (2007), pp. 76–81.

[9] B. Berge and J. Peseux, *Variable focal lens controlled by an external voltage: An application of electrowetting*, Eur. Phys. J. E, 3 (2000), pp. 159–163.

[10] M. Burger, *A framework for the construction of level set methods for shape optimization and reconstruction*, Interfaces Free Bound., 5 (2002), pp. 301–329.

[11] W. Bürger and E. Kuwert, *Area-minimizing disks with free boundary and prescribed enclosed volume*, J. Reine Angew. Math., 2008 (2008), pp. 1–27.

[12] P. Ciarlet, Jr., and C. Scheid, *Electrowetting of a 3D drop: Numerical modelling with electrostatic vector fields*, M2AN Math. Model. Numer. Anal., 44 (2010), pp. 647–670.

[13] R. Courant and N. Davids, *Minimal surfaces spanning closed manifolds*, Proc. Nat. Acad. Sci. USA, 26 (1940), pp. 194–199.

[14] P.-G. de Gennes, *Wetting: Statics and dynamics*, Rev. Modern Phys., 57 (1985), pp. 827–863.

[15] P.-G. de Gennes, F. Brochard-Wyart, and D. Quéré, *Capillarity and Wetting Phenomena: Drops, Bubbles, Pearls, Waves*, Springer-Verlag, New York, 2004.

[16] M. C. Delfour and J.-P. Zolésio, *Shapes and Geometries: Analysis, Differential Calculus, and Optimization*, Adv. Des. Control 4, SIAM, Philadelphia, 2001.

[17] G. Doğan, P. Morin, R. H. Nochetto, and M. Verani, *Discrete gradient flows for shape optimization and applications*, Comput. Methods Appl. Mech. Engrg., 196 (2007), pp. 3898–3914.

[18] G. Dziuk, *An algorithm for evolutionary surfaces*, Numer. Math., 58 (1990), pp. 603–611.

[19] J. Elschner, J. Rehberg, and G. Schmidt, *Optimal regularity for elliptic transmission problems including C^1 interfaces*, Interfaces Free Bound., 9 (2007), pp. 233–252.

[20] A. Epstein, *Bioinspired, Dynamic, Structured Surfaces for Biofilm Prevention*, Ph.D. thesis, Harvard University, 2012.

[21] A. K. Epstein, A. I. Hochbaum, P. Kim, and J. Aizenberg, *Control of bacterial biofilm growth on surfaces by nanostructural mechanics and geometry*, Nanotechnology, 22 (2011), 494007.

[22] L. C. Evans, *Partial Differential Equations*, AMS, Providence, RI, 1998.

[23] R. B. Fair, V. Srinivasan, H. Ren, P. Paik, V. K. Pamula, and M. G. Pollack, *Electrowetting-based on-chip sample processing for integrated microfluidics*, in Proceedings of the IEEE International Electron Devices Meeting (IEDM), 2003.

[24] R. S. Falk and S. W. Walker, *A mixed finite element method for EWOD that directly computes the position of the moving interface*, SIAM J. Numer. Anal., 51 (2013), pp. 1016–1040.

[25] M. M. Fall, *Embedded disc-type surfaces with large constant mean curvature and free boundaries*, Commun. Contemp. Math., 14 (2012), 1250037.

[26] R. Finn, *Equilibrium Capillary Surfaces*, Grundlehren Math. Wiss. 284, Springer, Berlin, 1986.

[27] D. Gilbarg and N. S. Trudinger, *Elliptic Partial Differential Equations of Second Order*, Springer, New York, 2001.

[28] M. Gonuguntla and A. Sharma, *Polymer patterns in evaporating droplets on dissolving substrates*, Langmuir, 20 (2004), pp. 3456–3463.

[29] R. D. Gulliver, *Regularity of minimizing surfaces of prescribed mean curvature*, Anna. of Math., 97 (1973), pp. 275–305.

[30] A. Henrot and M. Pierre, *Variation et optimisation de formes: Une analyse géométrique*, Math. Appl. (Berlin) 48 Springer, Berlin, 2005.

[31] M. HINTERMÜLLER AND A. LAURAIN, *A shape and topology optimization technique for solving a class of linear complementarity problems in function space*, Comput. Optim. Appl., 46 (2010), pp. 535–569.

[32] M. HINTERMÜLLER AND A. LAURAIN, *Optimal shape design subject to elliptic variational inequalities*, SIAM J. Control Optim., 49 (2011), pp. 1015–1047.

[33] M. HINZE, R. PINNAU, M. ULBRICH, AND S. ULBRICH, *Optimization with PDE Constraints*, Math. Model. Theory Appl. 23, Springer, New York, 2009.

[34] L. HOU, N. R. SMITH, AND J. HEIKENFELD, *Electrowetting manipulation of any optical film*, Appl. Phys. Lett., 90 (2007).

[35] K. ITO AND K. KUNISCH, *Lagrange Multiplier Approach to Variational Problems and Applications*, Adv. Des. Control, SIAM, Philadelphia, 2008.

[36] J. JOST, *Embedded minimal disks with a free boundary on a polyhedron in $\mathbb{R}^3$*, Math. Z., 199 (1988), pp. 311–320.

[37] H. KASUMBA AND K. KUNISCH, *On free surface pde constrained shape optimization problems*, Appl. Math. Comput., 218 (2012), pp. 11429–11450.

[38] H. KASUMBA, K. KUNISCH, AND A. LAURAIN, *A bilevel shape optimization problem for the exterior bernoulli free boundary value problem*, Interfaces Free Bound., 16 (2014), pp. 459–487.

[39] J.-H. KIM, S. I. AHN, J. H. KIM, J. S. KIM, K. CHO, J. C. JUNG, T. CHANG, M. REE, AND W.-C. ZIN, *Evaporation of sessile droplets of dilute aqueous solutions containing sodium n-alkylates from polymer surfaces: Influences of alkyl length and concentration of solute*, Langmuir, 24 (2008), pp. 11442–11450.

[40] A. KLINGNER AND F. MUGELE, *Electrowetting-induced morphological transistions of fluid microstructures*, J. Appl. Phys., 95 (2004), pp. 2918–2920.

[41] H.-M. KWON, J. C. BIRD, AND K. K. VARANASI, *Increasing leidenfrost point using micro-nano hierarchical surface structures*, Appl. Phys. Lett., 103 (2013), 201601.

[42] E. LANDESMAN AND A. LAZER, *Nonlinear perturbations of linear elliptic boundary value problems at resonance*, Indiana Univ. Math. J., 19 (1970), pp. 609–623.

[43] A. LAURAIN AND K. STURM, *Domain Expression of the Shape Derivative and Application to Electrical Impedance Tomography*, Technical report 1863, Weierstrass Institute for Applied Analysis and Stochastics, 2013.

[44] M. O. LAVRENTOVICH, J. H. KOSCHWANEZ, AND D. R. NELSON, *Nutrient shielding in clusters of cells*, Phys. Rev. E, 87 (2013), 062703.

[45] P. LEVKIN, *Biofunctional Polymer Surfaces*, Levkin Research Group, Karlsruhe Institute of Technology, 2013.

[46] Z. LIN, *Evaporative Self-Assembly of Ordered Complex Structures*, World Scientific, River Edge, NJ, 2012.

[47] N. G. MEYERS, *An L^p-estimate for the gradient of solutions of second order elliptic divergence equations*, Ann. Scu. Norm. Sup. Pisa (3), 17 (1963), pp. 189–206.

[48] J. MONNIER, P. WITOMSKI, P. CHOW-WING-BOM, AND C. SCHEID, *Numerical modeling of electrowetting by a shape inverse approach*, SIAM J. Appl. Math., 69 (2009), pp. 1477–1500.

[49] J. D. MOORE AND T. SCHULTE, *Minimal disks and compact hypersurfaces in euclidean space*, Proc. Amer. Math. Soc., 94 (1985), pp. 321–328.

[50] F. MUGELE AND J.-C. BARET, *Electrowetting: From basics to applications*, J. Phys. Condensed Matter, 17 (2005), pp. R705–R774.

[51] F. MURAT AND J. SIMON, *Sur le contrôle par un domaine géométrique*, Technical report, Laboratoire d'Analyse Numérique de l'Université Paris 6, 1976.

[52] A. NAKAJIMA, *Design of hydrophobic surfaces for liquid droplet control*, NPG Asia Materials, 3 (2011), pp. 49–56.

[53] R. H. NOCHETTO AND S. W. WALKER, *A hybrid variational front tracking-level set mesh generator for problems exhibiting large deformations and topological changes*, J. Comput. Phys., 229 (2010), pp. 6243–6269.

[54] C. QUILLIET AND B. BERGE, *Electrowetting: a recent outbreak*, Current Opinion Colloid Interface Sci., 6 (2001), pp. 34–39.

[55] L. D. RENNER AND D. B. WEIBEL, *Physicochemical regulation of biofilm formation*, MRS Bull., 36 (2011), pp. 347–355.

[56] A. ROS AND R. SOUAM, *On stability of capillary surfaces in a ball*, Pacific J. Math, 178 (1997), pp. 345–361.

[57] C. SCHEID AND P. WITOMSKI, *A proof of the invariance of the contact angle in electrowetting*, Math. Comput. Modelling, 49 (2009), pp. 647–665.

[58] J. D. Smith, R. Dhiman, S. Anand, E. Reza-Garduno, R. E. Cohen, G. H. McKinley, and K. K. Varanasi, *Droplet mobility on lubricant-impregnated surfaces*, Soft Matter, 9 (2013), pp. 1772–1780.

[59] K. M. Smyth, A. T. Paxson, H.-M. Kwon, and K. K. Varanasi, *Visualization of contact line motion on hydrophobic textures*, Surface Innovations, 1 (2013), pp. 84–91.

[60] J. Sokolowski and J.-P. Zolésio, *Introduction to Shape Optimization*, Springer Ser. in Comput. Math., Springer-Verlag, New York, 1992.

[61] K. Steffen and H. Wente, *The non-existence of branch points in solutions to certain classes of plateau type variational problems*, Math. Z., 163 (1978), pp. 211–238.

[62] M. Struwe, *The existence of surfaces of constant mean curvature with free boundaries*, Acta Math., 160 (1988), pp. 19–64.

[63] J. I. Toivanen, J. Haslinger, and R. A. E. Mäkinen, *Shape optimization of systems governed by Bernoulli free boundary problems*, Comput. Methods Appl. Mech. Engrg., 197 (2008), pp. 3803–3815.

[64] J. I. Toivanen, J. Haslinger, and R. A. E. Mäkinen, *Topology optimization in Bernoulli free boundary problems*, J. Engrg Math., (2012), pp. 1–16.

[65] F. Tröltzsch, *Optimal Control of Partial Differential Equations*, Grad. Stud. Math., AMS, Providence, RI, 2010.

[66] S. W. Walker, *FELICITY: Finite Element Implementation and Computational Interface Tool for You*, http://www.mathworks.com/matlabcentral/fileexchange/31141-felicity.

[67] S. W. Walker, *A Hybrid Variational-Level Set Approach to Handle Topological Changes*, M.S. thesis, University of Maryland, College Park, 2007.

[68] S. W. Walker, *Modeling, Simulating, and Controlling the Fluid Dynamics of Electro-Wetting on Dielectric*, Ph.D. thesis, University of Maryland, College Park, 2007.

[69] S. W. Walker, *A mixed formulation of a sharp interface model of stokes flow with moving contact lines*, ESAIM Math. Model. Numer. Analy., 48 (2014), pp. 969–1009.

[70] S. W. Walker, A. Bonito, and R. H. Nochetto, *Mixed finite element method for electrowetting on dielectric with contact line pinning*, Interfaces Free Bound., 12 (2010), pp. 85–119.

[71] S. W. Walker and E. E. Keaveny, *Analysis of shape optimization for magnetic microswimmers*, SIAM J. Control Optim., 51 (2013), pp. 3093–3126.

[72] S. W. Walker and B. Shapiro, *A control method for steering individual particles inside liquid droplets actuated by electrowetting*, Lab on a Chip, 5 (2005), pp. 1404–1407.

[73] S. W. Walker and B. Shapiro, *Modeling the fluid dynamics of electrowetting on dielectric (EWOD)*, J. Microelectromechanical Syst., 15 (2006), pp. 986–1000.

[74] S. W. Walker, B. Shapiro, and R. H. Nochetto, *Electrowetting with contact line pinning: Computational modeling and comparisons with experiments*, Phys. of Fluids, 21 (2009), 102103.

[75] S. W. Walker and M. J. Shelley, *Shape optimization of peristaltic pumping*, J. Comput. Phys., 229 (2010), pp. 1260–1291.

[76] H. C. Wente, *A general existence theorem for surfaces of constant mean curvature*, Math. Z., 120 (1971), pp. 277–288.

[77] A. R. Wheeler, H. Moon, C.-J. Kim, J. A. Loo, and R. L. Garrell, *Electrowetting-based microfluidics for analysis of peptides and proteins by matrix-assisted laser desorption/ionization mass spectrometry*, Analytical Chemistry, 76 (2004), pp. 4833–4838.

[78] J. N. Wilking, T. E. Angelini, A. Seminara, M. P. Brenner, and D. A. Weitz, *Biofilms as complex fluids*, MRS Bull., 36 (2011), pp. 385–391.